significantly limits the number of cell lines that can be generated for target gene expression. Recently, several researchers attempted to develop single-vector–based tet-inducible lentiviral systems [21–24]. However, the large plasmid size and lack of antibiotic selectable markers in these systems made the generation of plasmid constructs, high titer lentiviral particles, and stably expressing transgenic cell lines difficult.

To overcome the limitations of the current single vector-based tet-inducible lentiviral systems, we generated a robust system that incorporates all the necessary components for tet-off gene expression, restriction enzyme treatment/ligation independent cloning system, and antibiotic selectable markers in a single lentiviral vector. This vector consists of a modified tet-response element composite promoter (TRE-Tight) followed by a Gateway cassette containing *att*R recombination sites flanking a *ccd*B gene and a chloramphenicol resistant gene, which allows for easy and rapid shuttling of the gene of interest into the vector. This vector also carries an improved version of the tet-controlled transactivator (tTA-advanced) and the blasticidin resistance gene, linked by the self-cleaving viral T2A peptide, under a ubiquitous promoter. In the present study, we examined 2 ubiquitous promoters commonly used in mammalian systems: the CMV promoter and the human polypeptide chain elongation factor 1 α (EF-1α) promoter, to determine which promoter is more efficient in hADMPCs. In addition, we also confirmed whether genetically modified hADMPCs maintained their stem cell properties following transduction with this single tet-off lentiviral vector. We examined the expression pattern of cell surface markers, as well as the cells' differentiation potential into adipocytes, chondrocytes, osteocytes, and neuronal cells. Our data demonstrated that hADMPCs transduced with our all-in-one lentiviral vector were effectively selected by blasticidin without affecting their stem cell properties, and transgene expression was strictly regulated by doxycycline (Dox) not only in undifferentiated cells but also in differentiated cells. A single tet-off lentiviral vector system thus provides a powerful tool for applied research on hADMPCs.

## Materials and Methods

### Adipose Tissue Samples

Subcutaneous adipose tissue samples (10–50 g each) were resected during plastic surgery in 5 women (age, 20–60 years) as excess discards. The study protocol was approved by the Review Board for Human Research of Kobe University Graduate School of Medicine, Foundation for Biomedical Research and Innovation, and Kinki University Pharmaceutical Research and Technology Institute (reference number: 10-005). Each subject provided signed informed consent.

### Cell Culture

hADMPCs were isolated as previously reported [1,11,25,26] and maintained in a medium containing 60% DMEM-low glucose, 40% MCDB-201 medium (Sigma Aldrich, St. Louis, MO, USA), 1× insulin-transferrin-selenium (Life technologies, Carlsbad, CA, USA), 1 nM dexamethasone (Sigma Aldrich, St. Louis, MO, USA), 100 mM ascorbic acid 2-phosphate (Wako, Osaka, Japan), 10 ng/mL epidermal growth factor (PeproTech, Rocky Hill, NJ, USA), and 5% fetal bovine serum. The cells were plated to a density of $5\times10^3$ cells/cm$^2$ on fibronectin-coated dishes, and the medium was replaced every 2 days.

### Plasmid Construction and Lentivirus Production

EGFP was cloned into a pENTR11 vector (Invitrogen) to create an entry vector, pENTR11-EGFP. To generate pTRE-RfA, the tet-responsive element (TRE) of the pTRE-Tight vector (Clontech, Mountain Veiw, CA, USA) and the Reading frame A (RfA), a Gateway cassette containing *att*R recombination sites flanking a *ccd*B gene and a chloramphenicol-resistance gene (Invitrogen) were introduced into *Xba*I-*Xho*I sites of pSico (Addgene plasmid 11578). An improved version of the tet-controlled transactivator (tTA-advanced: pTet-off-advanced Clontech) was linked to the blasticidin resistance (Bsd) gene by the viral T2A peptide to generate tTA-2A-Bsd. Briefly, 2A-Bsd was amplified by PCR using the following primers:

2A-Bsd F: GGGGGATCCGGCGAGGGCAGAGGAAGTCTTCTAACATGCGGTGACGTGGAGGAAAATCCCGGGCCCATGAAGACCTTCAACATCTCTCAG, Bsd R: GCGAGATCTTTAGTTCCTGGTGTACTTG. The resultant product was confirmed by sequencing and ligation with the SmaI site of tTA. EF promoter/CMV promoter and tTA-2A-Bsd was introduced into pTRE-RfA to produce pTRE-RfA-EF-tTA-2A-Bsd or pTRE-RfA-CMV-tTA-2A-Bsd. The entry vector pENTR11-EGFP and pTRE-RfA-EF-tTA-2A-Bsd, pTRE-RfA-CMV-tTA-2A-Bsd, CSII-EF-RfA, or CSII-CMV-RfA (kindly provided by Dr. Miyoshi, RIKEN BioResource Center, Tsukuba, Japan) were incubated with LR clonase II enzyme mix (Invitrogen) to generate pTRE-EGFP-EF-tTA-2A-Bsd, pTRE-EGFP-CMV-tTA-2A-Bsd, CSII-EF-EGFP or CSII-CMV-EGFP. The resultant plasmid was mixed with packaging plasmids (pCAG-HIVg/p and pCMV-VSVG-RSV-Rev, kindly provided by Dr. Miyoshi) and transfected into 293T cells. The supernatant medium, which contained lentiviral vectors, was collected 2 days after transduction and concentrated by centrifugation (6000× *g*, 15 h, 4°C). Viral titers (transduction unit: TU) were determined by serial dilution on 293T cells and the percentage of EGFP positive cells was measured by Guava easyCyte 8HT flow cytometer (Merck-Millipore, Billerica, MA, USA).

### Plasmid Propagation in *E. coli*

DH5α (F-, Φ80dlacZΔM15, Δ(lacZYA-argF)U169, deoR, recA1, endA1, hsdR17(rK-, mK+), phoA, supE44, λ-, thi-1, gyrA96, relA1) were used for general purpose. To propagate plasmids containing the ccdB gene, One Shot® ccdB Survival™ 2 T1 Phage-Resistant (T1R) chemically competent *E. coli* (Invitrogen) were used.

### Western Blot Analysis

Cells were washed with ice-cold phosphate-buffered saline and lysed with M-PER Mammalian Protein Extraction Reagent (Thermo Scientific Pierce, Rockford, IL, USA). Equal amounts of proteins were separated by sodium dodecyl sulfate polyacrylamide gel electrophoresis, transferred to polyvinylidene fluoride membranes (Immobilon-P; Merck-Millipore), and probed with antibody against TetR (from Clontech). Horseradish peroxidase (HRP)-conjugated anti-mouse secondary antibody (Cell Signaling Technology, Danvers, MA, USA) was used as a probe, and immunoreactive bands were visualized with the Immobilon Western Chemiluminescent HRP substrate (Millipore). The band intensity was measured using ImageJ software.

### Flow Cytometry Analysis

hADMPCs were seeded at a density of $2\times10^4$ cells per well in 12-well culture plates and were transduced with CSII-EF-EGFP or CSII-CMV-EGFP at a multiplicity of infection (m.o.i.) of 25, 50,

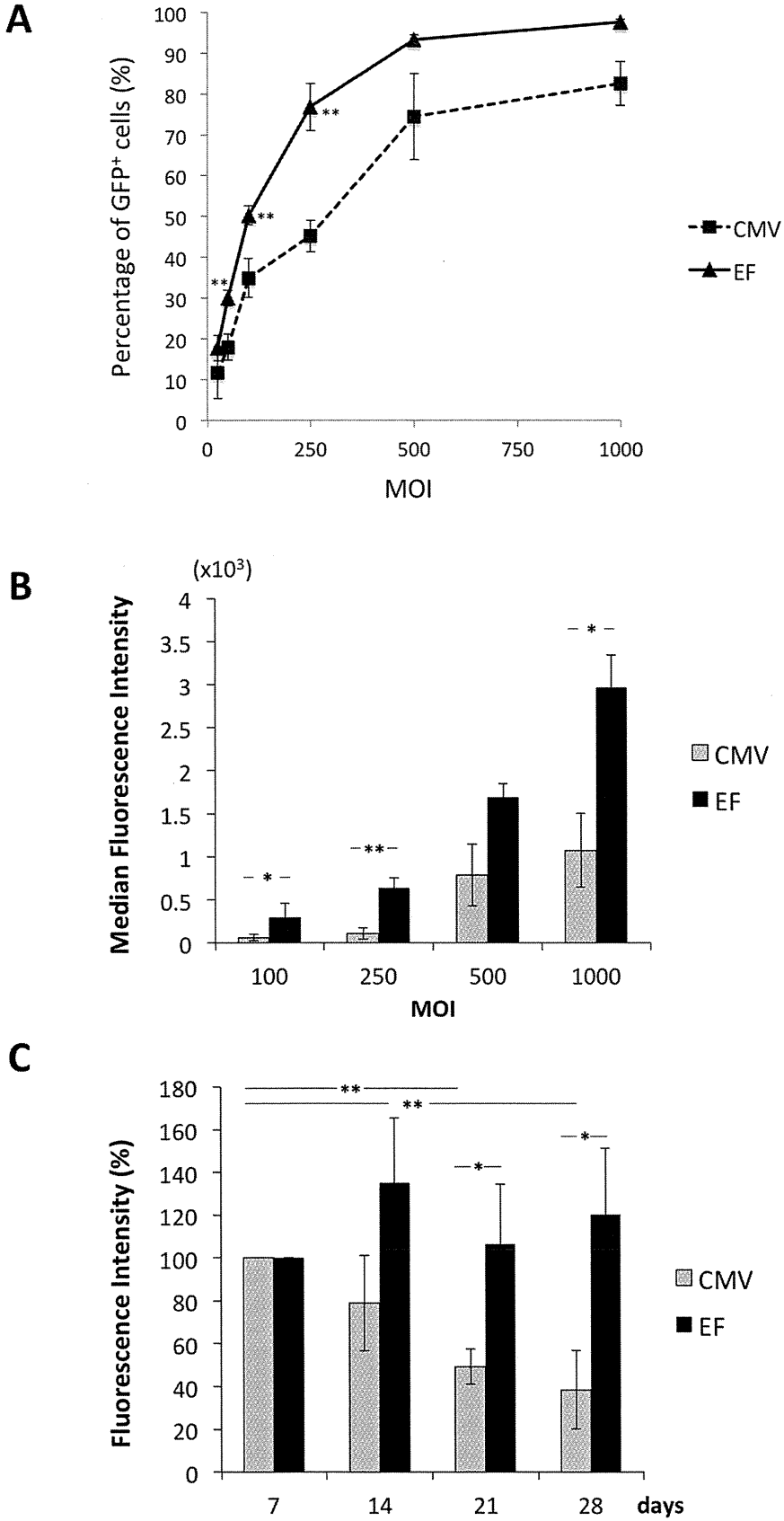


**Figure 1. The efficiency of CMV or EF-1α promoter in hADMPCs.** Lentiviral vectors encoding EGFP under the control of CMV or EF-1α promoter were transduced with hADMPCs at m.o.i. of 25, 50, 100, 250, 500, and 1000, and the cells were analyzed by flow cytometry. (A) The percentage of EGFP-positive hADMPCs transduced with CSII-CMV-EGFP (CMV) or CSII-EF-EGFP (EF). (B) (C) The median fluorescence intensities of the

EGFP-expressing populations. (B) hADMPCs transduced with CSII-CMV-EGFP or CSII-EF-EGFP at m.o.i. of 100, 250, 500, and 1000 were analyzed. (C) hADMPCs transduced with CSII-CMV-EGFP or CSII-EF-EGFP at m.o.i. of 1000 were analyzed over a 28 day period. Error bars represent the standard error of 3 independent analyses. **, P<0.01; *, P<0.05 (Student's t test).
doi:10.1371/journal.pone.0066274.g001

100, 250, 500, and 1000. Four days later, the cells were analyzed with a Guava easyCyte 8HT flow cytometer (Merck-Millipore) using an argon laser at 488 nm. Dead cells were excluded with the LIVE/DEAD fixable far red dead cell stain kit (Invitrogen). For analysis of hADMPCs transduced with pTRE-EGFP-EF-tTA-2A-Bsd or pTRE-EGFP-CMV-tTA-2A-Bsd, hADMPCs were transduced with the lentiviral vector at a m.o.i. of 250 and were cultured with or without 1 μg/mL Dox. Four days later, a part of the cells were analyzed with a Guava easyCyte 8HT flow cytometer. The rest of the cells were cultured with 4 μg/mL blasticidin and 1 μg/mL Dox for 3 weeks. Then, the cells were seeded in 6-well plates and cultured with or without Dox for 4 days. The cells were harvested and re-suspended in staining buffer (PBS containing 1% BSA, 2 mM EDTA, and 0.01% sodium azide) at a density of $1\times10^6$ cells/mL and incubated with phycoerythrin (PE)-conjugated antibody against CD13, CD29, CD34, CD44, CD73, CD90, CD105, or CD166 for 20 min. Non-specific staining was assessed using relevant isotype controls. 525/30 nm and 583/26 nm band pass filters were used for the detection of EGFP and PE, respectively. Dead cells were excluded with the LIVE/DEAD fixable far red dead cell stain kit (Invitrogen). FlowJo software (TreeStar Inc., Ashland, OR, USA) was used for quantitation analysis. The threshold for gating was determined as the fluorescence value above which less than 1% of the control cells were considered as positive events.

### Fluorescence Microscopy

Phase contrast and fluorescence images were obtained using Fluorescence Microscope (BZ-9000; Keyence, Osaka, Japan) using BZ Analyzer Software (Keyence).

### Adipogenic, Osteogenic, Chondrogenic, and Neurogenic Differentiation Procedures

For adipogenic differentiation, cells were cultured in differentiation medium (Zen-Bio, Durham, NC, USA). After 3 days, half of the medium was changed to adipocyte medium (Zen-Bio), and this was repeated every 3 days. Three weeks after differentiation, characterization of adipocytes was confirmed by microscopic observation of intracellular lipid droplets by oil red O staining. Osteogenic differentiation was induced by culturing the cells in DMEM containing 10 nM dexamethasone, 50 mg/dL ascorbic acid 2-phosphate, 10 mM β-glycerophosphate (Sigma), and 10% FBS. Differentiation was examined by alizarin red staining. For chondrogenic differentiation, $2\times10^5$ hADMPCs were centrifuged at 400× *g* for 10 min. The resulting pellets were cultured in chondrogenic medium (α-MEM supplemented with 10 ng/mL transforming growth factor-β, 10 nM dexamethasone, 100 mM ascorbate, and 1× insulin–transferrin–selenium solution) for 14 days, as described previously [27]. The pellets were fixed with 4% paraformaldehyde in PBS, embedded in OCT, frozen, and sectioned at 8 μm. The sections were incubated with PBSMT (PBS containing 0.1% Triton X-100, 2% skim milk) for 1 h at room temperature, and then incubated with mouse monoclonal antibody against type II collagen (Abcam, Cambridge, MA, USA) and rabbit polyclonal antibody against GFP (Invitrogen) for 1 h. After washing with PBS, cells were incubated with Alexa 546 conjugated anti-mouse IgG and Alexa 488 conjugated anti-rabbit IgG for chondrocytes (Invitrogen) or Alexa 546 conjugated anti-rabbit IgG and Alexa 488 conjugated anti-rat IgG (Invitrogen) for neuronal cells. The cells were counterstained with 4′-6-diamidino-2-phenylindole (DAPI) (Invitrogen) to identify cellular nuclei. For neurogenic differentiation, cells were cultured in Hyclone AdvanceSTEM neural differentiation medium (Thermo Scientific, South Logan, UT, USA) for 2 days. Differentiation was examined by immunofluorescent staining against β3-tubulin. Cells were fixed with 4% paraformaldehyde in PBS for 10 min at 4°C and then washed 3 times in PBS. Blocking was performed with PBSMT for 1 h at room temperature. The differentiated cells were incubated with rabbit monoclonal antibody against β3-tubulin (Cell Signaling Technologies, Danvers, MA, USA) and rat monoclonal antibody against GFP (Nacalai, Kyoto, Japan). After washing with PBS, cells were incubated with Alexa 546 conjugated anti-rabbit IgG and Alexa 488 conjugated anti-rat IgG (Invitrogen). The cells were counterstained with 4′-6-diamidino-2-phenylindole (DAPI) (Invitrogen) to identify cellular nuclei.

## Results

### The Efficiency of the EF-1α Promoter was Higher than that of the CMV Promoter in hADMPCs

To determine the efficiency of the EF-1α promoter and the CMV promoter, hADMPCs were transduced with CSII-EF-EGFP or CSII-CMV-EGFP at a m.o.i. of 25, 50, 100, 250, 500, and 1000 and analyzed by flow cytometry. As shown in Figure 1A, percentage of GFP-positive cells increased in a dose-dependent manner. Intriguingly, transduction efficiency of CSII-EF-EGFP was significantly higher than that of CSII-CMV-EGFP in hADMPCs (Figure 1A). Moreover, a higher induction level of GFP was observed under the EF-1α promoter than under the CMV promoter, based on the median fluorescent intensity (Figure 1B). Furthermore, GFP fluorescent intensities driven from the CMV promoter were significantly decreased (from 100% on day 7 to 49.3% on day 21 and 38.4% on day 28; Figure 1C), indicating that promoter silencing occurred as previously reported [19]. In contrast, hADMPCs transduced with CSII-EF-EGFP sustained GFP expression levels with no significant reduction throughout the 28-day experimental period (Figure 1C).

### Construction and Characterization of Dual-promoter Lentiviral Vectors in hADMPCs

Next, we constructed dual-promoter lentiviral vectors, which contain TRE-Tight followed by an improved version of tet-controlled transactivator (tTA advanced) induced under the CMV or EF-1α promoter (Figure 2A). In this "single tet-off lentiviral vector platform", the regulator and response elements are combined in a single lentiviral genome, along with a Gateway cassette containing *att*R recombination sites flanking a *ccd*B gene and a chloramphenicol-resistance gene, which allows an easy and rapid shuttling of the gene of interest into the vectors using the Gateway LR recombination reaction (Figure 2A). Using this system, we constructed pTRE-EGFP-CMV-tTA-2A-Bsd or pTRE-EGFP-EF-tTA-2A-Bsd (Figure 2B). Both the CMV and the EF-1α promoters drive the mRNA expression of tTA advanced linked to the Bsd gene by the Thosea asigna virus 2A (T2A) peptide sequence. This single transcript is then translated and cleaved into 2 proteins; tTA advanced carrying 2A tag at the

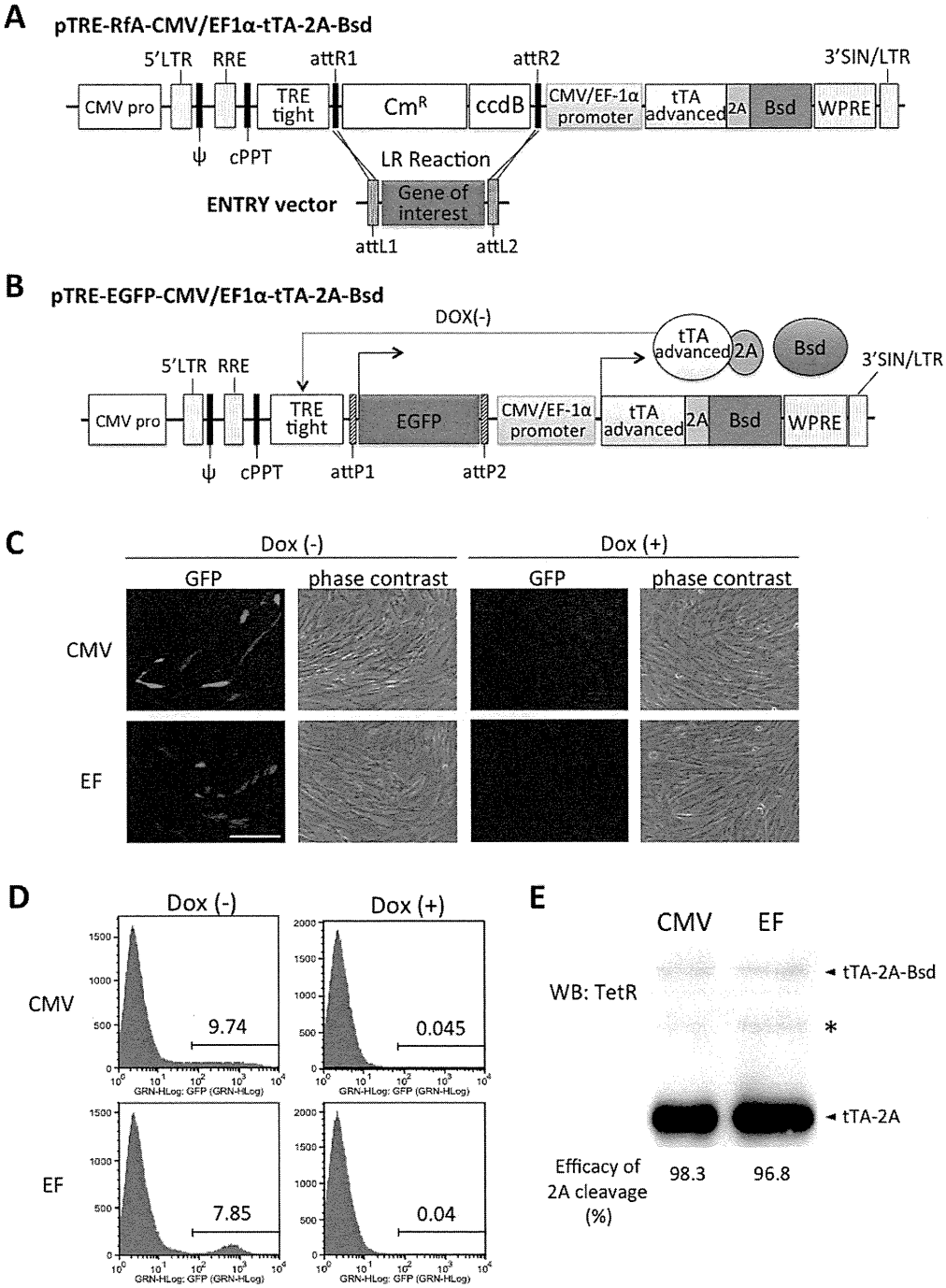


**Figure 2. Schematic drawings of the single lentiviral vectors for tet-off system used in this work.** (A) Gateway-compatible destination vectors containing *att*R recombination sites flanking a *ccd*B gene and a chloramphenicol-resistance gene, which allows an easy and rapid shuttling of gene of interest flanked by attL sites into the destination vectors using the Gateway LR recombination reaction. They also have an improved version of tetracycline-controlled transactivator (tTA) linked to the blasticidin resistant (Bsd) gene by the Thosea asigna virus 2A (2A) peptide sequence, whose expression is regulated by the CMV or EF-1α promoter. In the present study, we constructed an entry vector encoding EGFP flanked by attL, resulting in a destination clone, pTRE-EGFP-CMV-tTA-2A-Bsd or pTRE-EGFP-EF-tTA-2A-Bsd (B). In the absence of doxycycline (Dox), tTA-2A binds to the TRE-Tight promoter and activates EGFP transcription. For more details, see the Results section. CMV pro, CMV promoter; LTR, long terminal repeats; ψ, packaging signal; RRE, rev response elements; cPPT, central polypurine tract; TRE, tet-responsive element; $Cm^R$, chloramphenicol resistance; tTA, tetracycline-controlled transactivator; Bsd, blasticidin resistance; WPRE, woodchuck hepatitis virus posttranscriptional control element; SIN, self-inactivating. (C) (D) hADMPCs were transduced with pTRE-EGFP-CMV-tTA-2A-Bsd or pTRE-EGFP-EF-tTA-2A-Bsd at m.o.i. of 250. Four days after transduction, the cells were divided into 2 populations; with 1 μg/mL of Dox (Dox (+)) and without Dox (Dox (-)). (C) Fluorescent and phase contrast images. Scale bar, 200 μm. (D) Log fluorescence histograms of EGFP by flow cytometry analysis. (E) The whole cell lysates from hADMPCs transduced with pTRE-EGFP-CMV-tTA-2A-Bsd or pTRE-EGFP-EF-tTA-2A-Bsd were subjected to western blotting to monitor the cleavage efficiency of tTA-2A-Bsd proteins. A primary antibody against TetR was used to detect either tTA-2A-Bsd (non-cleaved form) or tTA-2A (cleaved form). Asterisk indicates a nonspecific band.

doi:10.1371/journal.pone.0066274.g002

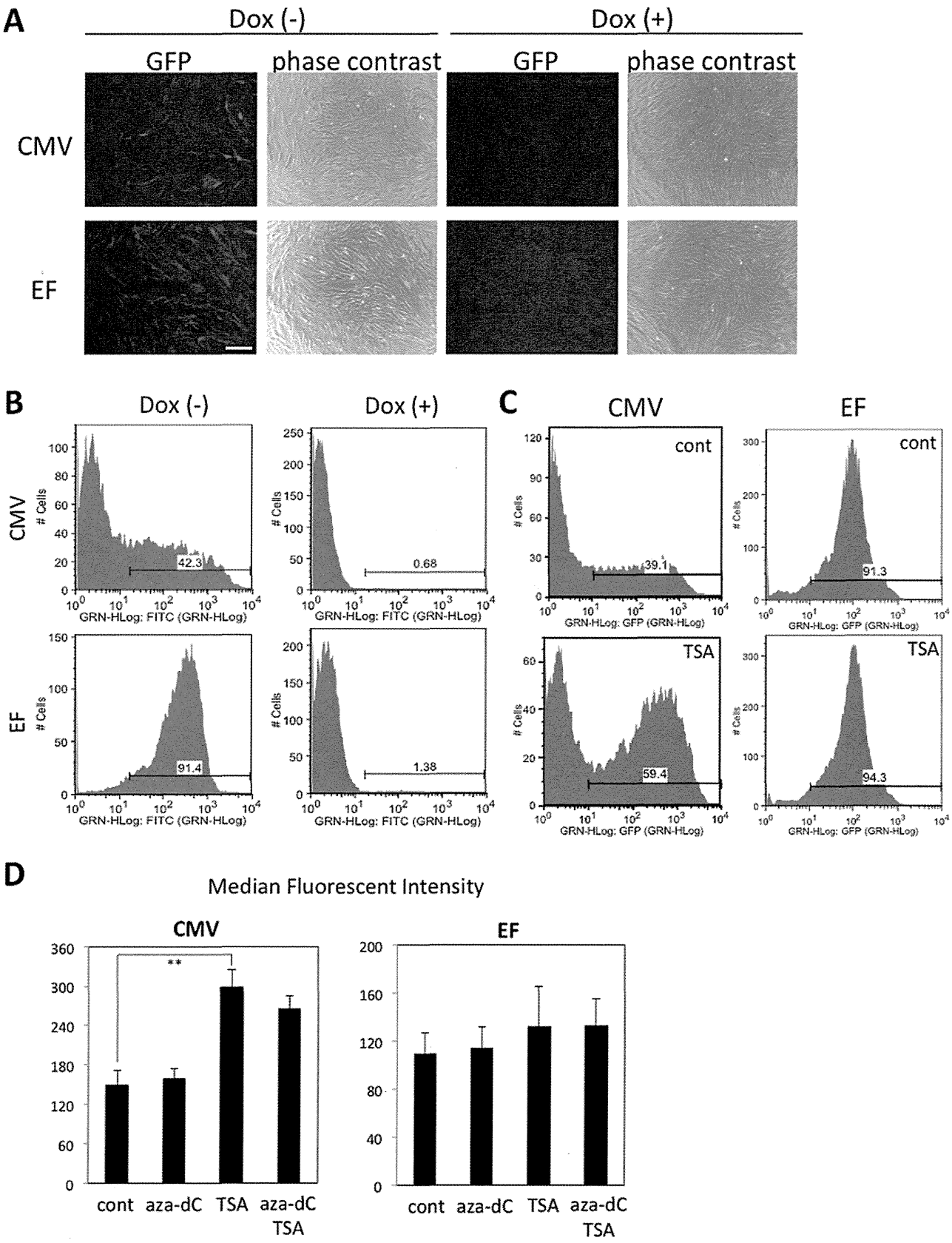


**Figure 3. Blasticidin selection of hADMPCs transduced with single tet-off lentiviral vector platform.** hADMPCs were transduced with pTRE-EGFP-CMV-tTA-2A-Bsd (CMV) or pTRE-EGFP-EF-tTA-2A-Bsd (EF) at m.o.i. of 250. The cells were treated with 4 μg/mL blasticidin and 1 μg/mL Dox for 2 weeks. Then, the cells were cultured in the absence (Dox (-)) or presence (Dox (+)) of 1 μg/mL Dox for 4 days, and analyzed under a microscope (A) and flow cytometer (B). The cells were treated with 100 nM TSA (TSA), 5 μM 5-aza-dC (aza-dC), or both for 48 h before analyzed by flow

cytometer. (C) A representative fluorescence histogram of EGFP. (D) The median fluorescence intensities of the EGFP-expressing populations. Error bars represent the standard error of 3 independent analyses. **, P<0.01 (Student's t test). Scale bar, 200 μm.
doi:10.1371/journal.pone.0066274.g003

C-terminus (tTA-2A) and Bsd. tTA-2A binds to the TRE-tight in the absence of Dox, a tet derivative, and activates transcription of EGFP to a very high level. In the presence of Dox, tTA-2A is unable to bind the TRE-Tight in a tet-responsive promoter, and the system is inactive.

To investigate the usefulness of these lentiviral vectors, hADMPCs were transduced with pTRE-EGFP-CMV-tTA-2A-Bsd or pTRE-EGFP-EF-tTA-2A-Bsd at a m.o.i. of 250. As shown in Figure 2C, expression of EGFP was observed in the absence of Dox, whereas addition of Dox (1 μg/mL) was enough to suppress the expression. Flow cytometry analysis revealed that the transduction efficiency was relatively low (EGFP-positive cells were 7.5~10%) compared with that of CSII-CMV-EGFP or CSII-EF-EGFP (EGFP-positive cells were 45% or 77% at a m.o.i. of 250, respectively; Figure 1A), and the tet-off system completely abolished gene expression in the presence of Dox (Figure 2D). Flow cytometry analysis also revealed that fluorescent intensity was relatively uniform in hADMPCs transduced with pTRE-EGFP-EF-tTA-2A-Bsd, but a wide range of fluorescent intensities was observed in hADMPCs infected with pTRE-EGFP-CMV-tTA-2A-Bsd. These data suggest that tTA-2A functions properly in this system. Moreover, western blot analysis against tTA showed the efficient cleavage (>95%) of tTA-2A-Bsd proteins into tTA-2A and Bsd (Figure 2E).

To further determine that Bsd cleaved from tTA-2A-Bsd was effective in this system, 4 μg/mL blasticidin was administered to hADMPCs. Within 1 week after the selection, control hADMPCs were completely killed (data not shown), whereas hADMPCs that were successfully transduced with either pTRE-EGFP-CMV-tTA-2A-Bsd or pTRE-EGFP-EF-tTA-2A-Bsd could survive and proliferate, demonstrating that Bsd from tTA-2A-Bsd is sufficient to confer blasticidin resistance to the cells. The surviving cells were kept in culture medium with blasticidin and then divided into 2 populations, either with Dox (1 μg/mL) or without Dox. As shown in Figure 3A and 3B, almost all (>90%) the cells transduced with pTRE-EGFP-EF-tTA-2A-Bsd strongly expressed EGFP in the absence of Dox. In hADMPCs transduced with pTRE-EGFP-CMV-tTA-2A-Bsd, however, >50% of the cells were EGFP negative regardless of their blasticidin resistance. Moreover, fluorescent intensities were quite variable; some cells expressed very high levels of EGFP, while others expressed very low levels (Figure 3A and 3B). This might be due to "promoter suppression," transcript repression of an upstream transcriptional unit by a downstream unit when 2 transcriptional units lie adjacent in head-to-tail tandem on a chromosome [28,29]. Studies have revealed that the suppression by adjacent units is epigenetic and involves modification of the chromatin structure, including DNA methylation at CpG sites within the promoter, histone deacetylation, histone methylation at specific residues (e.g., H3K9, H3K27), and densely packed nucleosomes that create a closed chromatin structure. In order to determine if inhibiting histone deacetylases or DNA methylation would re-induce EGFP expression, pTRE-EGFP-CMV-tTA-2A-Bsd cells were treated with histone deacetylase inhibitor trichostatin A (TSA) and/or DNA methylation inhibitor 5-aza-2′-deoxycytidine (5-aza-dC). TSA treatment significantly increased the number of EGFP-positive cells and strengthened the fluorescent intensities of EGFP, whereas 5-aza-dC had no effect, suggesting that EGFP expression was repressed by histone deacetylation when stably transduced with pTRE-EGFP-CMV-tTA-2A-Bsd (Figure 3C and 3D). These inhibitors had no effect on hADMPCs transduced with pTRE-EGFP-EF-tTA-2A-Bsd. These data suggest that the dual-promoter lentiviral vector using the EF promoter is more resistant to gene silencing than that using the CMV promoter.

### Blasticidin-selected hADMPCs Maintain the Properties of Their Parental hADMPCs

hADMPCs are an attractive material for cell therapy because of their ability to secrete various cytokines and growth factors. These cells also have the ability to differentiate into various types of cells, including adipocytes, chondrocytes, osteocytes, hepatocytes, cardiomyoblasts, and neuronal cells. Gene manipulation of hADMPCs may thus generate great possibilities for cell therapy and tissue engineering. From this point of view, the development of an efficient and stable Dox-responsive gene transfer system to achieve high levels of transgene expression in hADMPCs, without affecting the phenotype, is of special interest for the field. We therefore studied the cell properties of hADMPCs transduced with the single tet-off lentiviral vector after blasticidin selection. Flow cytometry analysis revealed no changes in the expression of the main surface markers (positive for CD13, CD29, CD44, CD73, CD90, CD105, and CD166, and negative for CD34) either in the absence or presence of Dox (Figure 4). To further confirm the properties of hADMPCs, the cells were differentiated into adipocytes, osteocytes, chondrocytes, and neuronal cells. As shown in Figure 5, blasticidin-selected hADMPCs maintained their ability to differentiate into adipocytes, osteocytes, chondrocytes, and neuronal cells. Moreover, EGFP was stably expressed in the differentiated cells only in the absence of Dox (Figure 5).

## Discussion

In recent years, there is growing interest in the use of MSCs for cell therapy and tissue engineering because of their differentiation potential and ability to secrete growth factors [7–11]. Furthermore, because of their hypo-immunogenicity and immune modulatory effects, MSCs are good candidates for gene delivery vehicles for therapeutic purposes [12,14]. In addition to primary MSCs, genetically modified MSCs have been applied to bone regeneration, muscle repair, diabetes, Parkinson's disease, and myocardial infarction recovery [14,30–35]. Duan et al. reported that the angiogenic effect of MSCs could be enhanced by adenovirus-mediated HGF overexpression in the treatment of cardiac ischemia injury [14]. Karnieli et al. and Li et al. both reported the reversal of hyperglycemia in streptozotocin-induced diabetic mice after transplantation of insulin-producing cells originating from genetically modified Pdx-1 expressing MSCs [32,33].

While significant progress has been made in the use of genetically modified MSCs for basic and applied research, the current methods for gene manipulation are still insufficient for some applications. Adenoviral vectors are commonly used for transient expression because they remain epichromosomal in the host cells, and their ability to transiently infect target cells minimizes the risk of insertional mutagenesis [36]. However, relatively brief transgene expression may limit the utility of this approach to tissue repair applications. On the other hand, lentiviral vectors, which are promising vectors for gene delivery in primary human cells, integrate into the host cell genome, which may be an appropriate strategy for tissue repair applications

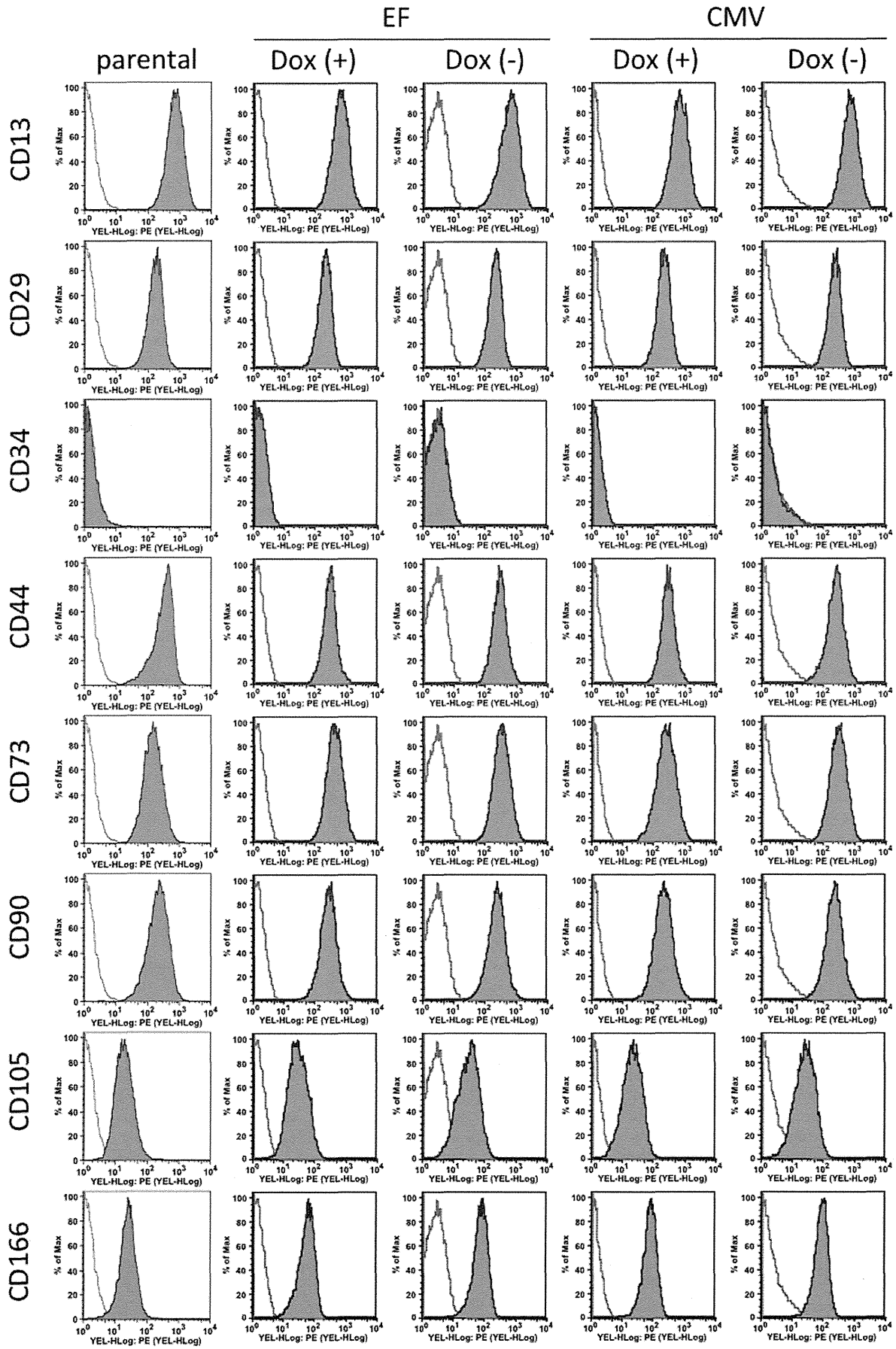
EF
CMV
parental
Dox (+)
Dox (-)
Dox (+)
Dox (-)
CD13
CD29
CD34
CD44
CD73
CD90
CD105
CD166
% of Max
YEL-HLog: PE (YEL-HLog)

**Figure 4. Expression pattern of surface cell markers on Dox-responsive hADMPCs.** Dox-responsive hADMPCs after selection by blasticidin were cultured in the absence (Dox(-)) or presence (Dox (+)) of 1 μg/mL Dox for 4 days. Expression of the different surface markers were analyzed by flow cytometry and compared to the expression by a parental hADMPCs. They were stained with PE-coupled antibodies against CD13, CD29, CD34, CD44, CD73, CD90, CD105, and CD166. Histogram of a PE-coupled mouse IgG1 κ isotype control is shown in gray. CMV; hADMPCs transduced with pTRE-EGFP-CMV-tTA-2A-Bsd, EF; hADMPCs transduced with pTRE-EGFP-EF-tTA-2A-Bsd.
doi:10.1371/journal.pone.0066274.g004

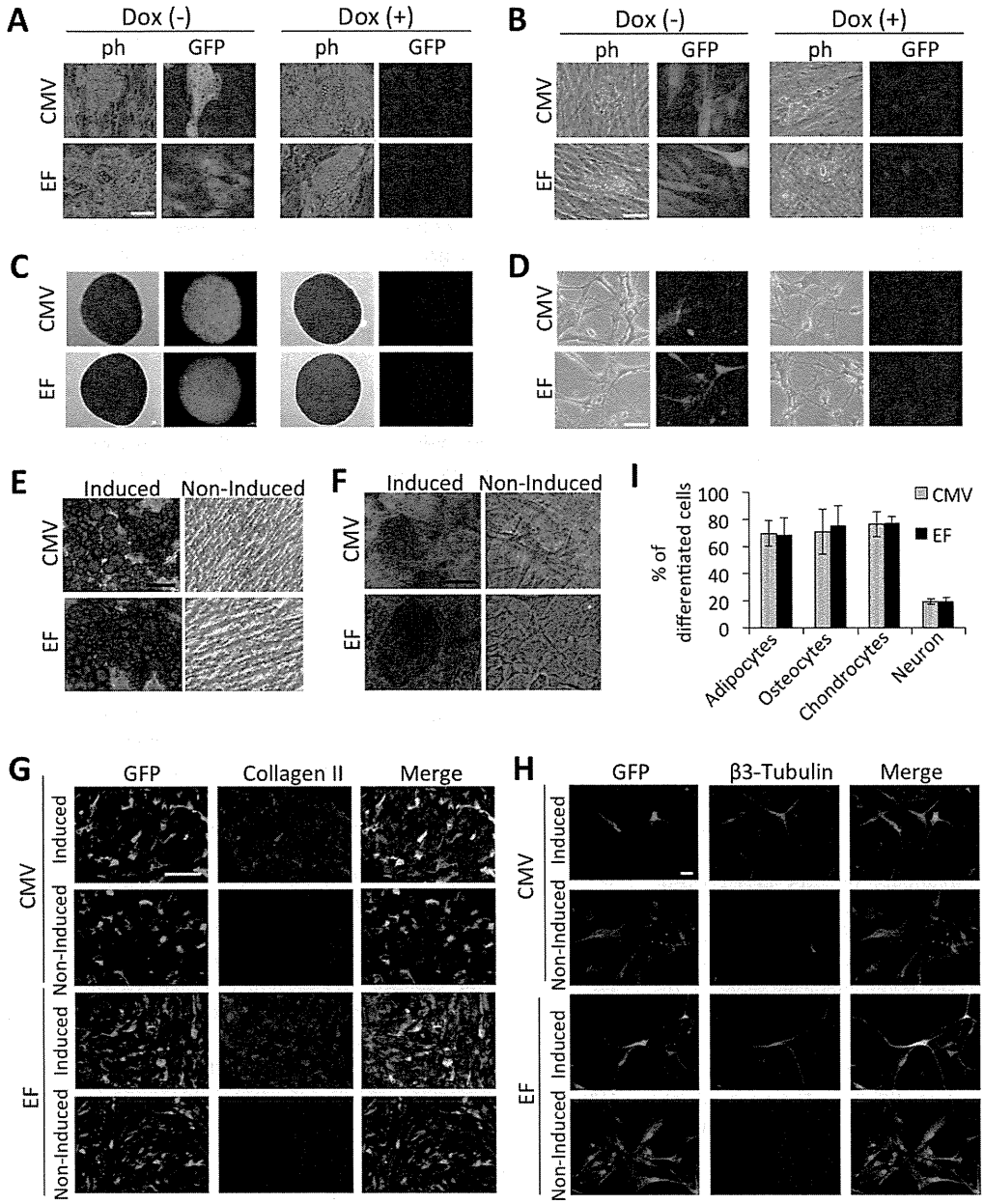


**Figure 5. Differentiation potential of Dox-responsive hADMPCs.** Dox-responsive hADMPCs were differentiated into adipocytes (A, E), osteocytes (B, F), chondrocytes (C, G), and neuronal cells (D, H). (A–D) Phase contrast (ph) and fluorescent (GFP) images. Dox-responsive hADMPCs were differentiated in the absence of Dox (Dox(−)) or in the presence of 1 μg/mL Dox (Dox(+)) as described in the material and methods section. (E–I) Confirmation of differentiated cells by oil red O staining for adipocytes (E), alizarin red staining for osteocytes (F), immunohistochemical staining against collagen II for chondrocytes (G), and immunohistochemical staining against β3-tubulin for neuronal cells (H). The percentages of differentiated cells to each cell type were calculated by the computerized image analysis (I). Cells that were not induced to differentiate (non-induced) were used as a negative control. CMV; hADMPCs transduced with pTRE-EGFP-CMV-tTA-2A-Bsd, EF; hADMPCs transduced with pTRE-EGFP-EF-tTA-2A-Bsd. Scale bar, 50 μm.
doi:10.1371/journal.pone.0066274.g005

requiring sustained, long-term expression of therapeutic proteins. In this study, we generated novel lentiviral vectors with a tet-off system, and demonstrated that our lentiviral vector systems were significantly effective and strictly regulated in hADMPCs, without affecting their stem cell properties.

Gene silencing is of considerable importance where stable, long-term expression is required. Researchers have reported that transgene silencing occurred when the CMV promoter was used in some cell types, especially in embryonic stem cells [15–17]. Since Kawabata et al. also demonstrated that virus-derived promoters inefficiently functioned in embryonic stem cells in gene transfer experiments [37], down-regulation and unsuitability of promoters in stem cells should be considered. Therefore, transduction efficacy and durability of transgene expression in hADMPCs is also an important issue to be determined. Qin et al. reported that the human EF-1α promoter and the TRE promoter are more efficient than the CMV promoter to drive lentiviral mediated transgene expression in rat bone marrow-derived MSCs [18]. McGinley et al. also showed that EF-1α and human phosphoglycerate kinase-1 (PGK) promoters have a clear advantage over the CMV promoter in transducing rat bone marrow-derived MSC transduction with lentivirus [19]. Consistent with their findings, our data also demonstrated that the EF-1α promoter was more efficient than the CMV promoter to drive EGFP expression in hADMPCs (Figure 1A, B). Moreover, a significant decrease in fluorescent intensity was observed by 28 days after transduction with lentiviral vector CSII-CMV-EGFP (Figure 1C), suggesting that the CMV promoter might be silenced in hADMPCs. We also demonstrated the intriguing finding that most (>90%) of the hADMPCs transduced with pTRE-EGFP-EF-tTA-2A-Bsd strongly expressed EGFP in the absence of Dox, whereas >50% of the cells transduced with pTRE-EGFP-CMV-tTA-2A-Bsd were EGFP negative, regardless of their blasticidin resistance (Figure 3A, B). Our data demonstrated that the inhibitor of histone deacetylation trichostatin A (TSA) re-induced the expression of EGFP (Figure 3C, D), suggesting that "promoter suppression" might occur by histone deacetylation, not by DNA methylation of CpG sites within the TRE tight promoter. "Promoter suppression" is a transcript repression of a 5′ transcriptional unit by a 3′ unit when 2 transcriptional units lie adjacent in head-to-tail tandem on a chromosome [28,29]. In this study, it is possible that the downstream unit of CMV-tTA-2A-Bsd repressed the upstream unit of TRE-EGFP because (1) resistance to blasticidin implies the transcriptional unit of CMV-tTA-2A-Bsd is active, and (2) reactivation of EGFP expression by TSA implies the transcriptional unit of TRE-EGFP is epigenetically silenced. In order to eliminate the promoter suppression or transcriptional interference between 2 transcriptional units, some researchers have been trying to separate the 2 units by polyadenylation, terminator, and insulator sequences [28,38]. However, these sequences extend the lentiviral vector size, which may affect the lentiviral titers produced from the vector. From this point of view, our finding that the transcriptional unit driven from the TRE tight promoter is resistant to gene silencing when arranged in tandem with the EF-tTA-2A-Bsd transcriptional unit (Figure 3) is of interest in the fields of both basic and clinical research, although the underlying mechanism remains elusive.

In general, large numbers of cells displaying the appropriate phenotypes are required for tissue engineering. Moreover, fully differentiated cells do not proliferate [39]. Therefore, in order to obtain enough cells to perform a transplant from genetically modified MSCs, it is important to develop a system in which the gene of interest is tightly regulated and inducible, and in which stably expressing transgenic cell lines can be obtained without affecting their stem cell properties. Using the system, MSCs transduced with lentiviral vectors can be selected and increased in numbers from a limited number of MSCs, before the target genes are induced. After obtaining an adequate number of gene-manipulated MSCs, the target genes could be induced in order to start differentiation. According to our data, hADMPCs transduced with pTRE-EGFP-EF-tTA-2A-Bsd were successfully selected by blasticidin, could proliferate, maintain their stem cell properties, and regulate EGFP expression tightly by Dox (Figure 4, 5), demonstrating that this all-in-one lentiviral vector is a promising gene delivery system for generating the material for artificial organs.

A major advantage of using the 2A cleavage factor in the construction of multi-cistronic vectors is its small size compared to internal promoter entry site (IRES) sequences. Because the titer of the lentivirus decreases with increasing size of the lentiviral vector, it is important to minimize the length of the sequences. In addition, linkage of 2 genes by 2A peptide resulted in efficient co-expression of the genes, whereas a gene placed downstream of an IRES is expressed at 2- to 3-fold lower levels than a gene placed upstream [40,41]. In this study, tTA-2A-Bsd cassette driven from CMV or EF-1α promoter showed ~90% cleavage (Figure 3). However, the point that should be considered is the effect of residual 2A peptide on the protein. As the processing occurred at the end of the 2A peptide, the 2A tag remains attached at the tTA C-terminus. Our data demonstrated that the presence of this extra 2A peptide did not seem to interfere with the activity of tTA since Dox strictly regulated the expression of EGFP under the control of TRE-tight promoter (Figure 2D, 3A, 3B and 5). Moreover, when Bsd is cleaved, an additional proline is attached at the N-terminus. We demonstrated that this did not affect a function of Bsd because hADMPCs transduced with either pTRE-EGFP-CMV-tTA-2A-Bsd or pTRE-EGFP-EF-tTA-2A-Bsd could survive and proliferate in medium containing blasticidin at a concentration at which all of the parental hADMPCs died.

Another advantage of our lentiviral system is the availability of a restriction enzyme treatment/ligation independent cloning system, called the Gateway system (Invitrogen). In general, the construction of lentiviral vectors using a conventional restriction enzyme/ligation cloning method has poor efficiency due to the large sizes and the lack of proper cloning sites. In our hands, cloning efficiency into our new lentiviral vectors pTRE-RfA-CMV-tTA-2A-Bsd or pTRE-RfA-EF-tTA-2A-Bsd using LR recombination reaches nearly 100%, saving time and effort in construction of the vectors. In addition, there are several resources available that take advantage of the Gateway vector. For example, CCSB Human ORFeome Collection (Dana-Farber Cancer Institute, Center for Cancer Systems Biology) represents almost 12,000 fully-sequenced cloned human ORFs which can be readily transferred to Gateway compatible destination vectors for various functional proteomics studies [42]. Block-iT pol II miR RNAi system from Invitrogen, which is designed to express artificial miRNAs, also enables compatibility with Gateway destination vectors for gene knock-down experiments [43].

In conclusion, our new single tet-off lentiviral vector system provides powerful tools not only for applied research on hADMPCs and other stem cells, but also basic research on a variety of cell lines and primary cells.

## Acknowledgments

We thank J. Uda, S. Tamura, C. Sone, K. Nakagita, and H. Isshi for technical support. We thank Dr. Tyler Jacks for providing the pSico plasmid and Dr. Hiroyuki Miyoshi for the CSII-EF-RfA, CSII-CMV-RfA, pCMV-VSVG-RSV-Rev, and pCAG-HIVg/p plasmids.

## Author Contributions

Conceived and designed the experiments: HM MM. Performed the experiments: HM MM KS HO AM. Analyzed the data: HM MM KS. Contributed reagents/materials/analysis tools: HM MM HO AI AM. Wrote the paper: HM MM TH.

## References


1. Okura H, Komoda H, Saga A, Kakuta-Yamamoto A, Hamada Y, et al. (2010) Properties of hepatocyte-like cell clusters from human adipose tissue-derived mesenchymal stem cells. Tissue engineering Part C, Methods 16: 761–770.
2. Okura H, Matsuyama A, Lee CM, Saga A, Kakuta-Yamamoto A, et al. (2010) Cardiomyoblast-like cells differentiated from human adipose tissue-derived mesenchymal stem cells improve left ventricular dysfunction and survival in a rat myocardial infarction model. Tissue engineering Part C, Methods 16: 417–425.
3. Okura H, Komoda H, Fumimoto Y, Lee CM, Nishida T, et al. (2009) Transdifferentiation of human adipose tissue-derived stromal cells into insulin-producing clusters. Journal of artificial organs : the official journal of the Japanese Society for Artificial Organs 12: 123–130.
4. Safford KM, Safford SD, Gimble JM, Shetty AK, Rice HE (2004) Characterization of neuronal/glial differentiation of murine adipose-derived adult stromal cells. Experimental neurology 187: 319–328.
5. Leu S, Lin YC, Yuen CM, Yen CH, Kao YH, et al. (2010) Adipose-derived mesenchymal stem cells markedly attenuate brain infarct size and improve neurological function in rats. Journal of translational medicine 8: 63.
6. Ikegame Y, Yamashita K, Hayashi S, Mizuno H, Tawada M, et al. (2011) Comparison of mesenchymal stem cells from adipose tissue and bone marrow for ischemic stroke therapy. Cytotherapy 13: 675–685.
7. Tan B, Luan Z, Wei X, He Y, Wei G, et al. (2011) AMP-activated kinase mediates adipose stem cell-stimulated neuritogenesis of PC12 cells. Neuroscience 181: 40–47.
8. Reid AJ, Sun M, Wiberg M, Downes S, Terenghi G, et al. (2011) Nerve repair with adipose-derived stem cells protects dorsal root ganglia neurons from apoptosis. Neuroscience.
9. Rehman J, Traktuev D, Li J, Merfeld-Clauss S, Temm-Grove CJ, et al. (2004) Secretion of angiogenic and antiapoptotic factors by human adipose stromal cells. Circulation 109: 1292–1298.
10. Lee EY, Xia Y, Kim WS, Kim MH, Kim TH, et al. (2009) Hypoxia-enhanced wound-healing function of adipose-derived stem cells: increase in stem cell proliferation and up-regulation of VEGF and bFGF. Wound repair and regeneration : official publication of the Wound Healing Society [and] the European Tissue Repair Society 17: 540–547.
11. Moriyama M, Moriyama H, Ueda A, Nishibata Y, Okura H, et al. (2012) Human adipose tissue-derived multilineage progenitor cells exposed to oxidative stress induce neurite outgrowth in PC12 cells through p38 MAPK signaling. BMC Cell Biol 13: 21.
12. Wu H, Ye Z, Mahato RI (2011) Genetically modified mesenchymal stem cells for improved islet transplantation. Mol Pharm 8: 1458–1470.
13. Pfeifer A, Ikawa M, Dayn Y, Verma IM (2002) Transgenesis by lentiviral vectors: lack of gene silencing in mammalian embryonic stem cells and preimplantation embryos. Proc Natl Acad Sci U S A 99: 2140–2145.
14. Duan HF, Wu CT, Wu DL, Lu Y, Liu HJ, et al. (2003) Treatment of myocardial ischemia with bone marrow-derived mesenchymal stem cells overexpressing hepatocyte growth factor. Mol Ther 8: 467–474.
15. Brooks AR, Harkins RN, Wang P, Qian HS, Liu P, et al. (2004) Transcriptional silencing is associated with extensive methylation of the CMV promoter following adenoviral gene delivery to muscle. J Gene Med 6: 395–404.
16. Kim S, Kim GJ, Miyoshi H, Moon SH, Ahn SE, et al. (2007) Efficiency of the elongation factor-1alpha promoter in mammalian embryonic stem cells using lentiviral gene delivery systems. Stem Cells Dev 16: 537–545.
17. Meilinger D, Fellinger K, Bultmann S, Rothbauer U, Bonapace IM, et al. (2009) Np95 interacts with de novo DNA methyltransferases, Dnmt3a and Dnmt3b, and mediates epigenetic silencing of the viral CMV promoter in embryonic stem cells. EMBO Rep 10: 1259–1264.
18. Qin JY, Zhang L, Clift KL, Hulur I, Xiang AP, et al. (2010) Systematic comparison of constitutive promoters and the doxycycline-inducible promoter. PLoS One 5: e10611.
19. McGinley L, McMahon J, Strappe P, Barry F, Murphy M, et al. (2011) Lentiviral vector mediated modification of mesenchymal stem cells & enhanced survival in an in vitro model of ischaemia. Stem Cell Res Ther 2: 12.
20. Weber W, Fussenegger M (2006) Pharmacologic transgene control systems for gene therapy. J Gene Med 8: 535–556.
21. Shi Q, Tian X, Zhao Y, Luo H, Tian Y, et al. (2011) Anti-arthritic effects of FasL gene transferred intra-articularly by an inducible lentiviral vector containing improved tet-on system. Rheumatol Int.
22. Wiederschain D, Wee S, Chen L, Loo A, Yang G, et al. (2009) Single-vector inducible lentiviral RNAi system for oncology target validation. Cell Cycle 8: 498–504.
23. Hioki H, Kuramoto E, Konno M, Kameda H, Takahashi Y, et al. (2009) High-level transgene expression in neurons by lentivirus with Tet-Off system. Neurosci Res 63: 149–154.
24. Benabdellah K, Cobo M, Munoz P, Toscano MG, Martin F (2011) Development of an all-in-one lentiviral vector system based on the original TetR for the easy generation of Tet-ON cell lines. PLoS One 6: e23734.
25. Okura H, Saga A, Fumimoto Y, Soeda M, Moriyama M, et al. (2011) Transplantation of human adipose tissue-derived multilineage progenitor cells reduces serum cholesterol in hyperlipidemic Watanabe rabbits. Tissue engineering Part C, Methods 17: 145–154.
26. Saga A, Okura H, Soeda M, Tani J, Fumimoto Y, et al. (2011) HMG-CoA reductase inhibitor augments the serum total cholesterol-lowering effect of human adipose tissue-derived multilineage progenitor cells in hyperlipidemic homozygous Watanabe rabbits. Biochemical and biophysical research communications 412: 50–54.
27. Okura H, Saga A, Fumimoto Y, Soeda M, Moriyama M, et al. (2011) Transplantation of human adipose tissue-derived multilineage progenitor cells reduces serum cholesterol in hyperlipidemic Watanabe rabbits. Tissue Eng Part C Methods 17: 145–154.
28. Villemure JF, Savard N, Belmaaza A (2001) Promoter suppression in cultured mammalian cells can be blocked by the chicken beta-globin chromatin insulator 5'HS4 and matrix/scaffold attachment regions. J Mol Biol 312: 963–974.
29. Emerman M, Temin HM (1986) Comparison of promoter suppression in avian and murine retrovirus vectors. Nucleic Acids Res 14: 9381–9396.
30. Tai K, Pelled G, Sheyn D, Bershteyn A, Han L, et al. (2008) Nanobiomechanics of repair bone regenerated by genetically modified mesenchymal stem cells. Tissue Eng Part A 14: 1709–1720.
31. Goudenege S, Pisani DF, Wdziekonski B, Di Santo JP, Bagnis C, et al. (2009) Enhancement of myogenic and muscle repair capacities of human adipose-derived stem cells with forced expression of MyoD. Mol Ther 17: 1064–1072.
32. Li Y, Zhang R, Qiao H, Zhang H, Wang Y, et al. (2007) Generation of insulin-producing cells from PDX-1 gene-modified human mesenchymal stem cells. J Cell Physiol 211: 36–44.
33. Karnieli O, Izhar-Prato Y, Bulvik S, Efrat S (2007) Generation of insulin-producing cells from human bone marrow mesenchymal stem cells by genetic manipulation. Stem Cells 25: 2837–2844.
34. Dezawa M, Kanno H, Hoshino M, Cho H, Matsumoto N, et al. (2004) Specific induction of neuronal cells from bone marrow stromal cells and application for autologous transplantation. J Clin Invest 113: 1701–1710.
35. Fan L, Lin C, Zhuo S, Chen L, Liu N, et al. (2009) Transplantation with survivin-engineered mesenchymal stem cells results in better prognosis in a rat model of myocardial infarction. Eur J Heart Fail 11: 1023–1030.
36. Ghosh SS, Gopinath P, Ramesh A (2006) Adenoviral vectors: a promising tool for gene therapy. Appl Biochem Biotechnol 133: 9–29.
37. Kawabata K, Sakurai F, Yamaguchi T, Hayakawa T, Mizuguchi H (2005) Efficient gene transfer into mouse embryonic stem cells with adenovirus vectors. Mol Ther 12: 547–554.
38. Tian J, Andreadis ST (2009) Independent and high-level dual-gene expression in adult stem-progenitor cells from a single lentiviral vector. Gene Ther 16: 874–884.
39. Clarke MF, Fuller M (2006) Stem cells and cancer: two faces of eve. Cell 124: 1111–1115.
40. Chinnasamy D, Milsom MD, Shaffer J, Neuenfeldt J, Shaaban AF, et al. (2006) Multicistronic lentiviral vectors containing the FMDV 2A cleavage factor demonstrate robust expression of encoded genes at limiting MOI. Virol J 3: 14.
41. Ibrahimi A, Vande Velde G, Reumers V, Toelen J, Thiry I, et al. (2009) Highly efficient multicistronic lentiviral vectors with peptide 2A sequences. Hum Gene Ther 20: 845–860.
42. Temple G, Gerhard DS, Rasooly R, Feingold EA, Good PJ, et al. (2009) The completion of the Mammalian Gene Collection (MGC). Genome Res 19: 2324–2333.
43. Liang Z, Wu H, Reddy S, Zhu A, Wang S, et al. (2007) Blockade of invasion and metastasis of breast cancer cells via targeting CXCR4 with an artificial microRNA. Biochem Biophys Res Commun 363: 542–546.

Stem Cell Reports
Resource
ISSCR
OPEN ACCESS

# Long-Term Self-Renewal of Human ES/iPS-Derived Hepatoblast-like Cells on Human Laminin 111-Coated Dishes

Kazuo Takayama,[1,2,3] Yasuhito Nagamoto,[1,2] Natsumi Mimura,[2] Katsuhisa Tashiro,[4] Fuminori Sakurai,[1] Masashi Tachibana,[1] Takao Hayakawa,[5] Kenji Kawabata,[4] and Hiroyuki Mizuguchi[1,2,3,6,*]
[1]Laboratory of Biochemistry and Molecular Biology, Graduate School of Pharmaceutical Sciences, Osaka University, Osaka 565-0871, Japan
[2]Laboratory of Hepatocyte Differentiation, National Institute of Biomedical Innovation, Osaka 567-0085, Japan
[3]iPS Cell-Based Research Project on Hepatic Toxicity and Metabolism, Graduate School of Pharmaceutical Sciences, Osaka University, Osaka 565-0871, Japan
[4]Laboratory of Stem Cell Regulation, National Institute of Biomedical Innovation, Osaka 567-0085, Japan
[5]Pharmaceutical Research and Technology Institute, Kinki University, Osaka 577-8502, Japan
[6]The Center for Advanced Medical Engineering and Informatics, Osaka University, Osaka 565-0871, Japan
*Correspondence: mizuguch@phs.osaka-u.ac.jp
http://dx.doi.org/10.1016/j.stemcr.2013.08.006


## SUMMARY

The establishment of self-renewing hepatoblast-like cells (HBCs) from human pluripotent stem cells (PSCs) would realize a stable supply of hepatocyte-like cells for medical applications. However, the functional characterization of human PSC-derived HBCs was not enough. To purify and expand human PSC-derived HBCs, human PSC-derived HBCs were cultured on dishes coated with various types of human recombinant laminins (LN). Human PSC-derived HBCs attached to human laminin-111 (LN111)-coated dish via integrin alpha 6 and beta 1 and were purified and expanded by culturing on the LN111-coated dish, but not by culturing on dishes coated with other laminin isoforms. By culturing on the LN111-coated dish, human PSC-derived HBCs were maintained for more than 3 months and had the ability to differentiate into both hepatocyte-like cells and cholangiocyte-like cells. These expandable human PSC-derived HBCs would be manageable tools for drug screening, experimental platforms to elucidate mechanisms of hepatoblasts, and cell sources for hepatic regenerative therapy.

## INTRODUCTION

Human embryonic stem cells (hESCs) and human induced pluripotent stem cells (hiPSCs) have the ability to self-replicate and to differentiate into all types of body cells including hepatoblasts and hepatocytes. Although cryopreserved primary human hepatocytes are useful in drug screening and liver cell transplantation, they rapidly lose their functions (such as drug metabolism capacity) and hardly proliferate in in vitro culture systems. On the other hand, human hepatic stem cells from fetal and postnatal human liver are able to self-replicate and able to differentiate into hepatocytes (Schmelzer et al., 2007; Zhang et al., 2008). However, the source of human hepatic stem cells is limited, and these cells are not available commercially. Therefore, the human pluripotent stem cell (hPSC)-derived hepatoblast-like cells (HBCs), which have potential to differentiate into the hepatocyte-like cells, would be an attractive cell source to provide abundant hepatocyte-like cells for drug screening and liver cell transplantation.

Because expandable and multipotent hepatoblasts or hepatic stem cells are of value, suitable culture conditions for the maintenance of hepatoblasts or hepatic stem cells obtained from fetal or adult mouse liver were developed (Kamiya et al., 2009; Tanimizu et al., 2004). Soluble factors, such as hepatocyte growth factor (HGF) and epidermal growth factor (EGF), are known to support the proliferation of mouse hepatic stem cells and hepatoblast (Kamiya et al., 2009; Tanimizu et al., 2004). Extracellular matrix (ECM) also affects the maintenance of hepatoblasts or hepatic stem cells. Laminin can maintain the character of mouse hepatoblasts (Dlk1-positive cells) (Tanimizu et al., 2004). However, the methodology for maintaining HBCs differentiated from hPSCs has not been well investigated. Zhao et al. (2009) have reported that hESC-derived hepatoblast-like cells (sorted N-cadherin-positive cells were used) could be maintained on STO feeder cells. Although a culture system using STO feeder cells for the maintenance of hepatoblast-like cells might be useful, there are two problems. The first problem is that N-cadherin is not a specific marker for human hepatoblasts. N-cadherin is also expressed in hESC-derived mesendoderm cells and definitive endoderm (DE) cells (Sumi et al., 2008). The second problem is that residual undifferentiated cells could be maintained on STO feeder cells. Therefore, their culture condition cannot rule out the possibility of the proliferation of residual undifferentiated cells. Because it is known that hPSC-derived cells have the potential to form teratomas in the host, the production of safer hepatocyte-like cells or hepatoblast-like cells has been required. Therefore, we decided to purify hPSC-derived HBCs, which can differentiate into mature hepatocyte-like cells, and then expand these cells.

In this study, we attempt to determine a suitable culture condition for the extensive expansion of HBCs derived

from hPSCs. We found that the HBCs derived from hPSCs can be maintained and proliferated on human laminin-111 (LN111)-coated dishes. To demonstrate that expandable, multipotent, and safe (i.e., devoid of residual undifferentiated cells) hPSC-derived HBCs could be maintained under our culture condition, the hPSC-derived HBCs were used for hepatic and biliary differentiation, colony assay, and transplantation into immunodeficient mice.

## RESULTS

### Human PSC-Derived Hepatoblast-like Cells Could Adhere onto Human LN111 via Integrin α6 and β1

The HBCs were generated from hPSCs (hESCs and hiPSCs) as described in Figure 1A (details of the characterization of hPSC-derived HBCs are described in Figure 3). Definitive endoderm differentiation of hPSCs was promoted by stage-specific transient transduction of FOXA2 in addition to the treatment with appropriate soluble factors (such as Activin A). Overexpression of FOXA2 is not necessary for establishing the hPSC-derived HBCs, but it is helpful for efficient generation of the hPSC-derived HBCs. On day 9, these hESC-derived populations contained two cell populations with distinct morphology (Figure 1B). One population resembled human hepatic stem cells that were isolated from human fetal liver (shown in red) (Schmelzer et al., 2007), whereas the other population resembled definitive endoderm cells (shown in green) (Hay et al., 2008). The population that resembled human hepatic stem cells was alpha-1-fetoprotein (AFP) positive, whereas the other population was AFP negative (Figure 1C, left). On day 9, the percentage of AFP-positive cells was approximately 80% (Figure 1C, right). To characterize these two cell populations (hESC-derived HBC and non-HBC [NHBC] populations), the colonies were manually isolated by using a pipette, and then the gene expression analysis was performed. The gene expression levels of *AFP*, *CD133*, *EpCAM*, *CK8*, and *CK18* in the hESC-derived HBCs were higher than those in the bulk population containing both hESC-derived HBCs and NHBCs (*CD133*, *EpCAM*, *CK8*, and *CK18* were named as pan-hepatoblast markers and are known to be strongly expressed in both human hepatic stem cells and hepatoblasts [Schmelzer et al., 2007; Zhang et al., 2008]) (Figure 1D). On the other hand, the gene expressions of *AFP*, *CD133*, *EpCAM*, *CK8*, and *CK18* in the hESC-derived NHBCs were hardly detected. The gene expression levels of DE, mesendoderm, and pluripotent markers in the hESC-derived NHBCs were higher than those in the hESC-derived HBCs, indicating that the hESC-derived NHBCs could remain in a more undifferentiated state than the hESC-derived HBCs (Figures S1A–S1C available online). These results suggest that hepatoblast-like cells could be differentiated from hPSCs.

To purify the hESC-derived HBCs, these cells were plated onto dishes coated with various laminins. There are 15 different laminin isoforms in human tissues. Although laminin is known to be useful to sustain mouse hepatoblasts (Tanimizu et al., 2004), it remains unknown which human laminin isoform has the potential to purify and expand the HBCs. To identify a human laminin isoform that would be useful for purifying hESC-HBCs, the hESC-HBCs and -NHBCs were plated onto dishes coated with various types of commercially available human laminins (Figure 1E). The hESC-derived HBCs could more efficiently adhere onto the human LN111-coated dish compared with hESC-derived NHBCs or unseparated populations (containing both HBCs and NBCs). These data suggest that a hESC-derived HBC population can be purified from the unseparated populations by culturing on human LN111-coated dishes. Because integrins are known to be important molecules for cell adhesion to the ECM including laminins, we expected that certain types of integrins would allow selective adhesion of the hESC-derived HBCs to human LN111-coated dish. The gene expression levels of various integrins were examined (Figure 1F). Among the integrin α subunits, the gene expression level of *integrin α6* in the hESC-derived HBCs was significantly higher than that in the hESC-derived NHBCs. In contrast, among the integrin β subunits, the gene expression level of *integrin β1* was higher than those of *integrin β2* and *β3* in all cell populations. The hESC-derived HBCs, but not NHBCs, expressed both integrin α6 and β1 (Figure S1D). Almost all adhesion of the hESC-derived HBCs to a human LN111-coated dish was inhibited by both function-blocking antibodies to integrin α6 and β1 (Figure 1G). These results indicated that the hESC-derived HBCs could attach to a human LN111-coated dish via integrin α6 and β1.

### The hPSC-Derived HBCs Could Be Proliferated and Maintained on a Human LN111-Coated Dish

To obtain the purified hESC-derived HBC population, the hESC-derived cells (day 9) were plated onto a human LN111-coated dish, and then unattached cells were removed at 15 min after plating (Figure 2A). Among various laminins, only human LN111 could proliferate (Figure 2B) and purify (Figure 2C) the AFP-positive population in the presence of HGF and EGF. During culture on the human LN111-coated dish, the morphology of the hESC-derived HBCs gradually changed into that of human hepatoblasts (Figure S1E) (Schmelzer et al., 2007). Therefore, the characteristics of hESC-derived HBCs might be changed by culturing on a human LN111-coated dish (details of the characterization of the hESC-derived HBCs are described in Figure 3). After culturing on a human LN111-coated

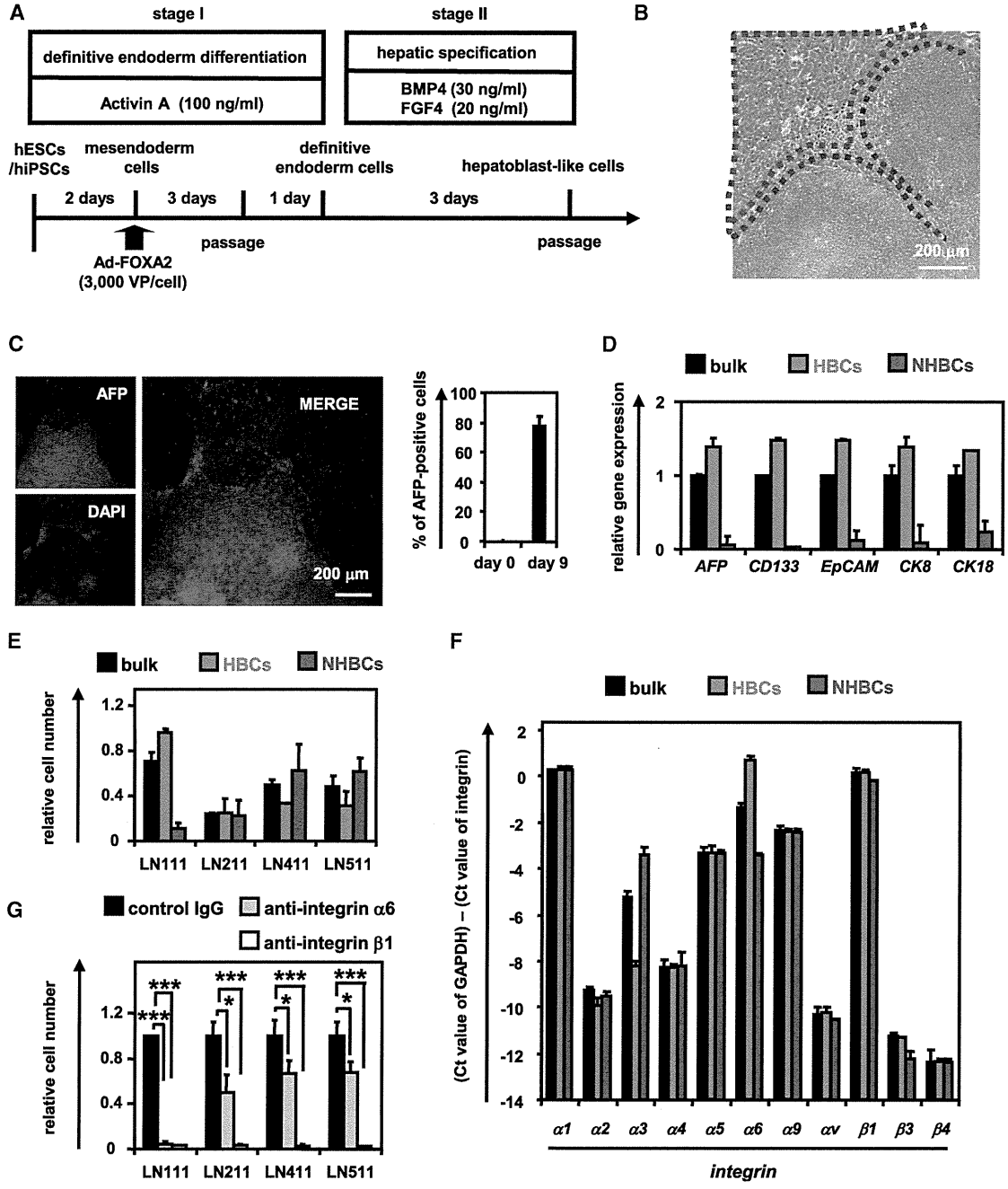


**Figure 1. The Human ESC-Derived HBCs Selectively Attached to a Human LN111-Coated Dish via Integrin α6 and β1**

(A) The procedure for the differentiation of hESCs (H9) into hepatoblast-like cells (HBCs) is presented schematically. Details are described in the Experimental Procedures.

(B) Phase-contrast micrographs of the hESC-derived HBCs (red) and non-HBCs (NHBCs) (green) are shown.

(C) The hESC-derived cells (day 9) were subjected to immunostaining with anti-AFP (red) antibodies. The percentage of AFP-positive cells was examined on day 0 or 9 by using FACS analysis. Data represent the mean ± SD from ten independent experiments. Cells on "day 0" and "day 9" were compared using Student's t test ($p < 0.01$).

(D) On day 9, the hESC-derived HBCs and NHBCs were manually picked, and the gene expression levels of *AFP* and pan-hepatoblast markers (*CD133*, *EpCAM*, *CK8*, and *CK18*) were measured by real-time RT-PCR. The gene expression levels of *AFP* and pan-hepatoblast markers in the hESC-derived cells (day 9; bulk) were taken as 1.0. Data represent the mean ± SD from four independent experiments. The gene expression levels in the HBCs were significantly different among the three groups (bulk, HBCs, and NHBCs) based on analysis with one-way ANOVA followed by Bonferroni post hoc tests ($p < 0.05$).

*(legend continued on next page)*

dish for a week, almost all of the cells were still AFP positive (Figures 2C and 2D). To characterize the cells cultured on various types of human laminins for 7 days, the gene expression levels of *AFP* and pan-hepatoblast (*CD133*, *CK8*, *CK18*, and *EpCAM*) markers were examined on day 16 (Figure 2E). The gene expression levels of *AFP* and pan-hepatoblast markers in the hESC-derived HBCs P1 (HBCs passaged once) did not change as compared with those of the hESC-derived HBCs (day 9; HBC P0) (the definitions of HBC P0, P1, P10, and clone in the present study are shown in Figure S3). The gene expression levels of mature hepatocyte and cholangiocyte markers in the hESC-derived HBC P1 did not change as compared with those of the hESC-derived HBC P0 (day 9) (Figure S1F). These results suggest that the characteristics of the hESC-derived HBC P1 are similar to those of the hESC-derived HBC P0, although their morphologies are quite different from each other. Interestingly, the gene expression levels of mature cholangiocyte markers in the cells cultured on human LN411- or 511-coated dishes were upregulated as compared with those of the hESC-derived HBC P0 (day 9) (Figure S1F), suggesting that human LN411 and 511 might promote biliary differentiation. Importantly, both hESC-derived HBCs and hiPSC-derived HBCs could extensively proliferate on a human LN111-coated dish for more than 15 passages (Figure 2F) in the presence of HGF and EGF. Doubling times of hESC (H9)-derived HBCs and hiPSC (Dotcom)-derived HBCs were approximately 78 and 67 hr, respectively. Almost all of the populations cultured on a human LN111-coated dish were AFP positive (Figure 2G). Taken together, these results suggested that the hPSC-derived HBCs would proliferate and be maintained on a human LN111-coated dish.

### Characterization of the hESC-Derived HBCs

To characterize the hESC-derived HBCs, the gene expression profiles in the hESC-derived purified HBCs (HBC P0), short-term cultured HBCs (HBCs passaged once [HBC P1]), and long-term cultured HBC (HBCs passaged ten times [HBC P10]) were examined. The hESC-derived HBCs were AFP positive (Figure 3A). Although the hESC-derived HBC P0 were negative for ALB, CK7, and CK19, the hESC-derived HBC P1 and P10 were positive for these genes (Figure 3A). Both integrin α6 and β1 (receptors of LN111) were strongly expressed in the hESC-derived HBC P0, P1, and P10 (Figure 3B). The gene expression levels of human hepatic stem cell markers (*N-CAM* and *Claudin 3* [Schmelzer et al., 2007]; these are not expressed in human hepatoblasts) in the hESC-derived HBC P0 were higher than those of the hESC-derived HBC P1 and P10 (Figure 3C). However, the gene expression level of *CK19* in the hESC-derived HBC P0 was lower than that of the hESC-derived HBC P1 and P10. The gene expression levels of pan-hepatoblast markers in the hESC-derived HBC P0 were similar to those of the hESC-derived HBC P1 and P10 (Figure 3D). The gene expression levels of human hepatoblast markers (*ALB*, *CYP3A7*, and *I-CAM* (Schmelzer et al., 2007), none of which were expressed in human hepatic stem cells) in the hESC-derived HBC P1 and P10 were higher than those of the hESC-derived HBC P0 (Figure 3E). However, the AFP expression level in the hESC-derived HBC P0 was similar to that of the hESC-derived HBC P1 and P10. Because the gene expression levels of mature hepatocyte and cholangiocyte markers in the hESC-derived HBC P1 and P10 were not increased as compared with those in the hESC-derived HBC P0 (Figure 3F), the hESC-derived HBC P1 and P10 were not segregated into either of the hepatic and biliary lineages. We also examined the gene expression levels of hepatoblast markers, which have been reported only in mice and not in humans (Figure 3G). The characteristics of the hPSC-derived HBCs are summarized in Figure S3. In addition, hESC-derived HBC P0 and HBC P10 showed normal karyotypes (Figure S2A). Therefore, the genetic stability of the HBCs was confirmed throughout the maintenance period. Taken together, these results suggest that the hESC-derived HBC P0 resemble human hepatic stem cells and the hESC-derived HBC P1 and P10 resemble human hepatoblasts, although some gene expression patterns in the hESC-derived HBCs differ from those in human hepatic stem cells and human hepatoblasts, respectively.

(E) The hESC-derived cells (day 9; bulk), HBCs, and NHBCs were plated onto human LN111-, 211-, 411-, or 511-coated dishes, and the attached cells were counted at 60 min after plating. The cell number that was initially plated was taken as 1.0. Data represent the mean ± SD from four independent experiments. The number of attached HBCs on LN111-coated dishes were significantly different among three groups (bulk, HBCs, and NHBCs) based on analysis with one-way ANOVA followed by Bonferroni post hoc tests ($p < 0.05$).

(F) The gene expression levels of the indicated integrins were measured in the hESC-derived cells (day 9; bulk), HBCs, and NHBCs by real-time RT-PCR. Data represent the mean ± SD from four independent experiments. The gene expression levels of *integrin α3* and *α6* in the HBCs were significantly different among three groups (bulk, HBCs, and NHBCs) based on analysis with one-way ANOVA followed by Bonferroni post hoc tests ($p < 0.05$).

(G) The adhesion of the hESC-derived HBCs to human LN111-, 211-, 411-, or 511-coated dishes was examined by using the indicated integrin antibodies. IgG antibodies were used as a control for uninhibited cell adhesion. The number of attached cells was estimated at 60 min after plating. The cell number in the control IgG-treated group was taken as 1.0. Data represent the mean ± SD from three independent experiments. "Control IgG" and "anti-integrin α6 or integrin β1" were compared using Student's t test. *$p < 0.05$; ***$p < 0.001$. See also Figure S1 and Tables S2–S5.

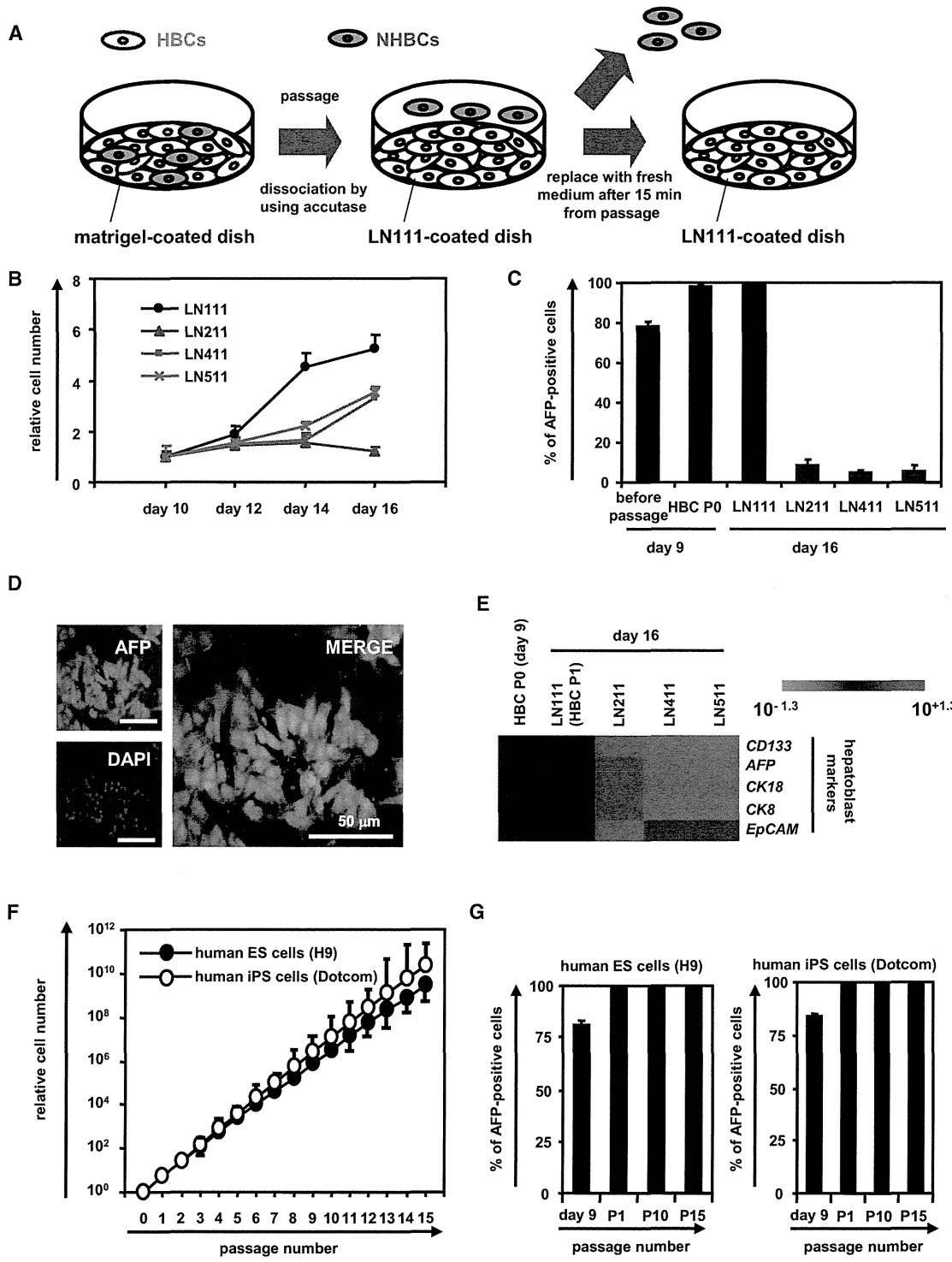


**Figure 2. The hESC-Derived HBCs Could Be Proliferated and Maintained on a Human LN111-Coated Dish**

(A) The hESC (H9)-derived cells (day 9) were plated onto a human LN111-coated dish. At 15 min after plating, the unattached cells were removed.

(B) The hESC (H9)-derived cells (day 9) were plated onto a human LN111, 211, 411, or 511-coated dish, and then the cell number were counted on days 10, 12, 14, and 16. The cell number on day 10 was taken as 1.0. Data represent the mean ± SD from three independent experiments. "LN111" was significantly different among four groups (LN111, 211, 411, and 511) on day 14 and 16 based on analysis with one-way ANOVA followed by Bonferroni post hoc tests ($p < 0.05$).

*(legend continued on next page)*

In order to examine whether the hESC-derived HBC P0 have the potential to proliferate clonally on various types of human laminins, single HBCs were plated on separate wells of a human LN111-coated 96-well plate at a low density (one cell per one well) (Table S1). Single cells that attached to the human LN111-coated dish were AFP positive and HNF4α positive (Figure S2B). At 7 days after plating, the hESC-derived HBC colonies (albumin [ALB]- and cytokeratin 7 [CK7] double positive) (a representative colony is shown in Figure S2C) were efficiently generated from the hESC-derived HBC P0 on a LN111-coated dish. Taken together, these results showed that the hESC-derived HBCs could be generated from both the hESC-derived HBC P0 population and the single hESC-derived HBC P0.

### The hPSC-Derived HBCs Could Differentiate into Both Hepatic and Biliary Lineages In Vitro

To examine whether the hESC-derived HBCs have the potential to differentiate into both hepatic and biliary lineages, first, these cells were differentiated into hepatocyte-like cells as described in Figure 4A. After 2 weeks of hepatic differentiation, almost all of the cells were polygonal in shape (Figure 4B) and were CYP3A4, αAT, and ALB positive (Figure 4C). The gene expression levels of mature hepatocyte markers in the HBC P0-, HBC P10-, or HBC clone-derived hepatocyte-like cells were higher than those in the cells that had not undergone hepatic differentiation (Figure 4D), although the gene expression levels of mature cholangiocyte markers in these cells did not change (Figure 4E). The ASGR1-positive cells in the HBC P0-, HBC P10-, and HBC clone-derived population accounted for approximately 60%, 90%, and 90% of the total, respectively (Figure 4F). The HBC P0-, HBC P10-, or HBC clone-derived hepatocyte-like cells had the ability to produce ALB (Figure 4G, left) and urea (Figure 4G, right). Next, the hESC-derived HBCs were differentiated into cholangiocyte-like cells as described in Figure 4H. After 2 weeks of biliary differentiation, tubular structures (Figure 4I) that were CK7 positive (Figure 4J) were observed. Although the gene expression levels of mature hepatocyte markers (Figure 4K) in the HBC P0-, HBC P10-, or HBC clone-derived cholangiocyte-like cells did not change, the gene expression levels of mature cholangiocyte markers (Figure 4L) in these cells were higher than those in the cells that had not undergone differentiation. Similar results were obtained by using another hESC line (H1) and hiPSC line (Dotcom) (Figure S4). Moreover, HBC-derived hepatocyte-like cells exhibited CYP metabolism capacity (Figure S5A) and a functional urea cycle that could response to ammonia (Figure S5B) and were considered to have potential to be applied in the prediction of drug-induced hepatotoxicity (Figure S5C). Taken together, these results indicated that the hPSC-derived HBCs have the ability to differentiate into both hepatic and biliary lineages in vitro.

### In Vivo Cell Transplantation Assays of the hPSC-Derived HBCs

To examine whether the hESC-derived HBCs could be used for hepatocyte transplantation, these cells were transplanted into $CCl_4$-treated immunodeficient mice as shown in Figure 5A. The hepatocyte functionality of the hESC-derived HBC P0 or HBC P10 was assessed by measuring secreted human ALB levels in the recipient mice (Figure 5B). Although human ALB was detected in the mice that were transplanted with the hESC-derived HBC P0 or HBC P10, it was not detected in the mice that were not transplanted with these cells. The ALB-positive cells were observed in mice transplanted with the hESC-derived HBC P0 or HBC P10 (Figure 5C). Most of the ALB-positive cells in mice transplanted with the hESC-derived HBC P10 were AFP negative (Figure 5D), indicating that transplanted hESC-derived HBCs were differentiated into mature hepatocyte-like cells (some of them were binuclear [Figure 5E, white arrows]). These results demonstrated that hESC-derived HBCs have the potential to be applied for hepatocyte transplantation.

(C) The hESC-derived cells (day 9) were plated onto a human LN111, 211, 411, or 511-coated dish. The percentage of AFP-positive cells was examined by using FACS analysis on day 9 (before passage and after passage [HBC P0]) or day 16. Data represent the mean ± SD from three independent experiments.

(D) The hESC-derived cells cultured on a human LN111-coated dish for 7 days were subjected to immunostaining with anti-AFP (green) antibodies.

(E) The hESC-derived cells (day 9) were plated onto human LN111, 211, 411, or 511-coated dishes. The gene expression levels of *AFP* and pan-hepatoblast markers (*CD133*, *EpCAM*, *CK8*, and, *CK18*) were measured by real-time RT-PCR on day 16. The gene expression levels in the hESC-derived HBCs (the LN111-attached cells were collected at 15 min after plating) were taken as 1.0.

(F) The HBCs derived from hESCs (H9) or hiPSCs (Dotcom) were cultured and cell growth was analyzed by obtaining a cell count at each passage. Data represent the mean ± SD from three independent experiments.

(G) The percentage of AFP-positive cells was examined by using FACS analysis on day 9 (before passage), P1 (HBCs passaged once), P10 (HBCs passaged ten times), and P15 (HBCs passaged 15 times). Data represent the mean ± SD from seven independent experiments.

See also Tables S2 and S3.

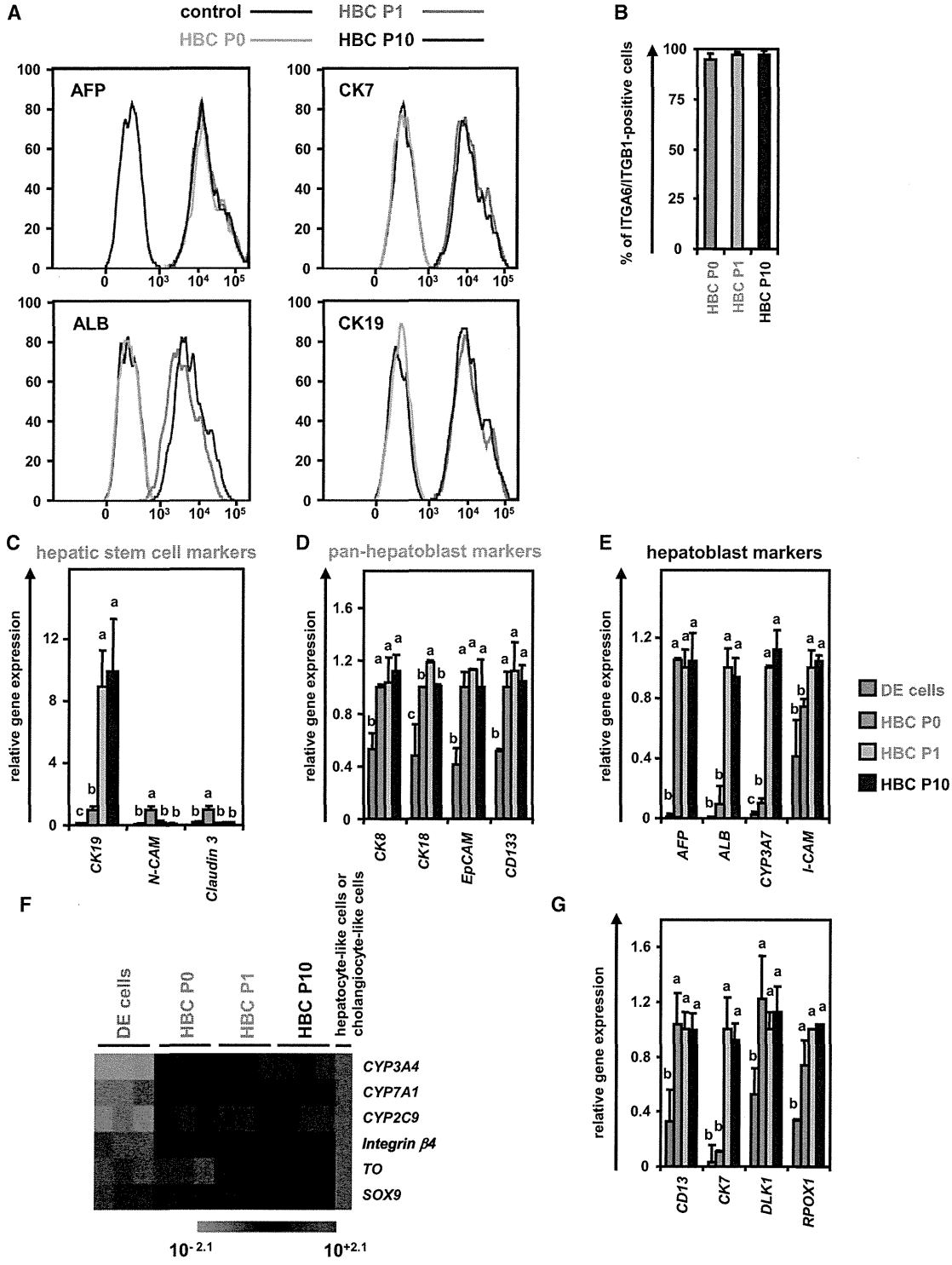


**Figure 3. The hESC-Derived HBCs Were Characterized**

(A and B) The hESCs (H9) were differentiated according to Figure 1A and then passaged onto a human LN111-coated dish. The attached cells (hESC-derived HBCs [HBC P0]) were collected at 15 min after plating. The percentage of AFP-positive, ALB-positive, CK7-positive, CK19-positive (A), and integrin α6- and integrin β1-double positive (B) cells in the hESC-derived HBC P0, HBC P1 (HBCs passaged once), and HBC P10 (HBCs passaged ten times) populations was estimated by using FACS analysis. Data represent the mean ± SD from seven independent experiments.

*(legend continued on next page)*

## DISCUSSION

The main purpose of this study was to establish and characterize expandable HBCs from hPSCs. First, we identified that human LN111 could support self-renewal and proliferation of hPSC-derived HBCs in the presence of HGF and EGF. Second, we showed that the hPSC-derived HBCs have the potential to segregate into both hepatic and biliary lineages, and to integrate into the mouse liver parenchyma.

We have demonstrated that the hPSC-derived HBCs could be maintained on a human LN111-coated dish in an integrin α6- and β1-dependent manner (Figure 1). It is known that undifferentiated hPSCs could be maintained on a human LN511-coated dish but not on a human LN111-coated dish (Rodin et al., 2010). This might suggest that human LN111 has the potential not only to selectively maintain HBCs, but also to eliminate residual undifferentiated cells. Our hepatoblast-like cells could efficiently proliferate for more than 3 months on a human LN111-coated dish (Figure 2). In the human liver development (during 5–10 weeks gestation), laminin is observed in both the perisinusoidal space and portal tracts (Couvelard et al., 1998). The expression of laminin is localized around the periportal biliary trees during the later stage of liver development (Couvelard et al., 1998). Hepatic stem cells reside around the hepatic portal area (Clément et al., 1988). It is also known that laminin is accumulated around oval cells although laminin is not expressed around quiescent mature hepatocytes (Paku et al., 2001). These facts suggest that laminin plays an important role in the maintenance and proliferation of hepatoblasts.

The hPSC-derived HBC P10 and clone were positive for hepatoblast markers (AFP, ALB, CYP3A7, and I-CAM), but negative for hepatic stem cell markers (N-CAM and Claudin 3) (Figure 3) (Schmelzer et al., 2007). Although the hPSC-derived HBCs were able to expand on human LN111-coated dish, Schmelzer et al. showed that human hepatoblasts do not proliferate under a monolayer culture condition, but human hepatic stem cells could self-replicate for more than 6 months (Schmelzer et al., 2007). Although further investigations of the hepatoblast characteristics in the hPSC-derived HBCs will be needed in the future, the results in the present study suggest that the characteristics of hPSC-derived HBCs expanded on human LN111-coated dishes were similar to those in human hepatoblasts isolated from the human liver (Schmelzer et al., 2007; Zhang et al., 2008).

The hPSC-derived HBCs had the ability to integrate into the mouse liver parenchyma (Figure 5), in the manner of human hepatic stem cells or hepatoblasts (Schmelzer et al., 2007). The human ALB serum levels (approximately 20–70 ng/ml) in mice transplanted with the hESC-derived HBC P0 or HBC P10 were comparable to those in the previous paper in which the hESC-derived definitive endoderm cells, hepatoblasts, and hepatocyte-like cells were transplanted into mice (Liu et al., 2011), but were lower than those of human liver chimeric mice (Tateno et al., 2004). Human ALB serum levels would increase if more suitable host mice, such as urokinase plasminogen activator-SCID mice were used (Tateno et al., 2004).

In this study, we have developed a technology for the maintenance and proliferation of hPSC-derived HBCs by using human LN111. To transplant these cells for purposes of regenerative medicine, a xeno-free culture condition for hPSC-derived HBCs must be developed in the future. It is hoped that the hPSC-derived HBCs and their derivatives will be helpful in various medical applications, such as drug screening and regenerative medicine.

## EXPERIMENTAL PROCEDURES

### hESC and hiPSC Culture

The hESC lines (H1 [WA01] and H9 [WA09] [WiCell Research Institute]) and the hiPSC line, Dotcom (JCRB number: JCRB1327) (Makino et al., 2009; Nagata et al., 2009), were maintained on a feeder layer of mitomycin-C-treated mouse embryonic fibroblasts (Millipore) with ReproStem medium (ReproCELL) supplemented with 5 and 10 ng/ml fibroblast growth factor 2 (FGF2) (Katayama Kagaku Kogyo), respectively. H1 and H9 were used following the Guidelines for Derivation and Utilization of Human Embryonic Stem Cells of the Ministry of Education, Culture, Sports, Science and Technology of Japan, and, furthermore, the study was approved by an independent ethics committee.

### In Vitro Hepatoblast Differentiation

The differentiation protocol for the induction of definitive endoderm cells and hepatoblasts was based on our previous report with some modifications (Inamura et al., 2011; Takayama et al., 2012a, 2012b, 2013). In mesendoderm differentiation, hESCs/iPSCs were

(C–F) The gene expression levels of hepatic stem cell markers (C), pan-hepatoblast markers (D), hepatoblast markers (E), and mature hepatocyte (*CYP3A4*, *7A1*, *2C9*, and *TO*) or cholangiocyte markers (*integrin β4* and *SOX9*) (F) were measured in the definitive endoderm cells, HBC P0, HBC P1, or HBC P10 by real-time RT-PCR.

(G) The gene expression levels of *CD13*, *CK7*, *DLK1*, and *PROX1* were measured in the hESC-derived definitive endoderm cells, HBC P0, HBC P1, or HBC P10 by real-time RT-PCR. Data represent the mean ± SD from three independent experiments. Statistical significance was evaluated by ANOVA followed by Bonferroni post hoc tests to compare four groups (DE cells, HBC P0, HBC P1, and HBC P10). Groups that do not share the same letter are significantly different from each other ($p < 0.05$). DE, definitive endoderm cells.

See also Figures S2 and S3 and Tables S2–S4.

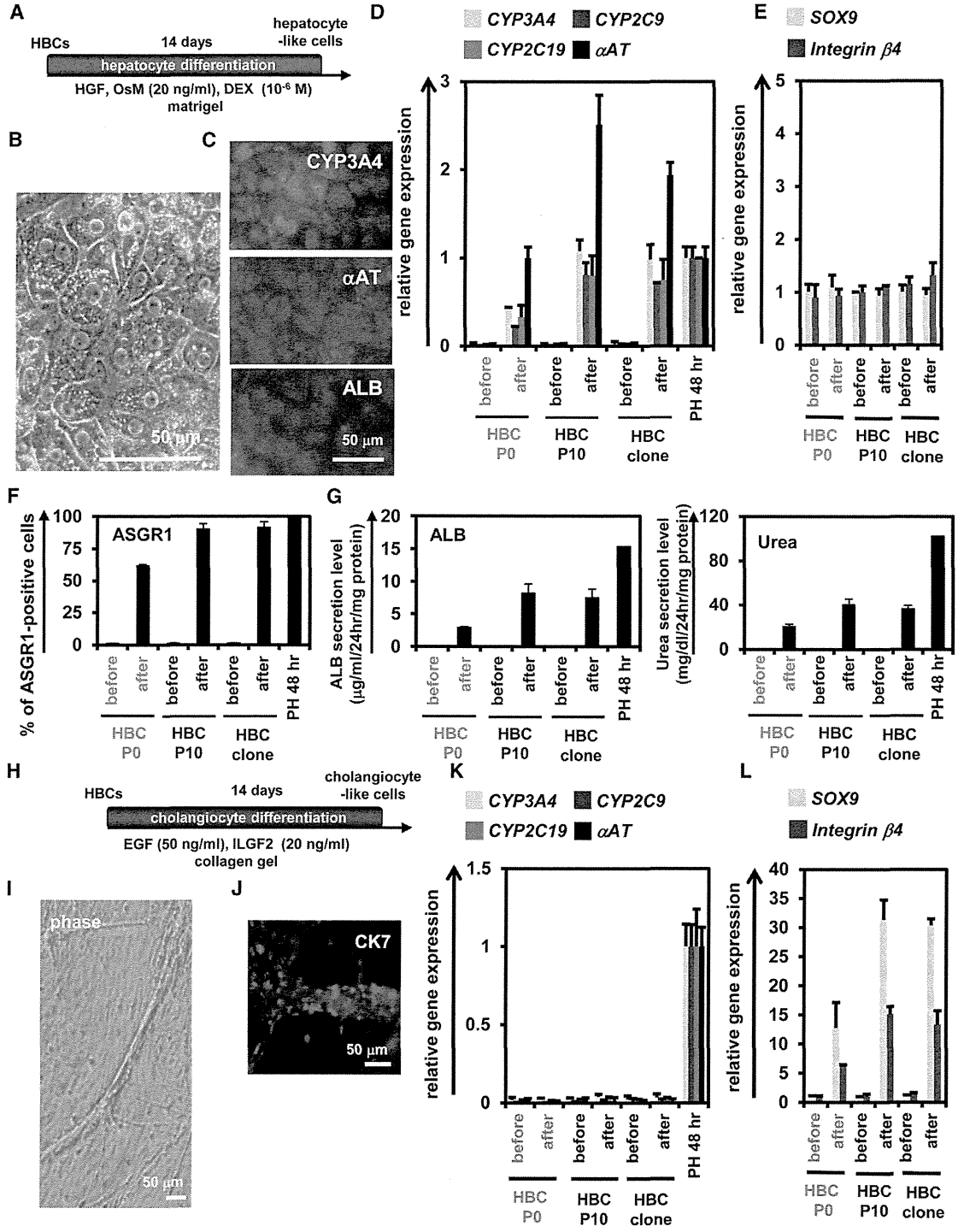


**Figure 4. The hESC-Derived HBCs Could Differentiate into Both Hepatic and Biliary Lineages**

(A) The procedure for differentiation of the hESC (H9)-derived HBC P0, HBC P10, or HBC clone into the hepatocyte-like cells is presented schematically. Details are described in Experimental Procedures.

(B) Phase-contrast micrographs of the HBC P10-derived hepatocyte-like cells are shown.

(C) The HBC P10-derived hepatocyte-like cells were subjected to immunostaining with anti-CYP3A4 (green), anti-αAT (red), and anti-ALB (red) antibodies.

(D and E) The gene expression levels of hepatocyte (D) or cholangiocyte (E) markers in HBC P0-, HBC P10-, or HBC clone-derived hepatocyte-like cells were measured by real-time RT-PCR after 14 days of hepatocyte differentiation. In (D), the gene expression levels in

*(legend continued on next page)*

cultured for 2 days on Matrigel (BD Biosciences) in differentiation hESF-DIF medium that contains 100 ng/ml Activin A (R&D Systems) (hESF-DIF medium was purchased from Cell Science & Technology Institute; differentiation hESF-DIF medium was supplemented with 10 μg/ml human recombinant insulin, 5 μg/ml human apotransferrin, 10 μM 2-mercaptoethanol, 10 μM ethanolamine, 10 μM sodium selenite, and 0.5 mg/ml bovine fatty acid free serum albumin [all from Sigma]). To generate definitive endoderm cells, the mesendoderm cells (day 2) were transduced with 3,000 vector particle (VP)/cell of FOXA2-expressing adenovirus vectors (Ad-FOXA2) for 1.5 hr and cultured until day 6 on Matrigel in differentiation hESF-DIF medium supplemented with 100 ng/ml Activin A. For induction of hepatoblasts, the definitive endoderm cells were cultured for 3 days on a Matrigel in differentiation hESF-DIF medium supplemented with 30 ng/ml bone morphogenetic protein 4 (BMP4) (R&D Systems) and 20 ng/ml FGF4 (R&D Systems).

### Establishment and Maintenance of the hPSC-Derived HBCs

The hPSC-derived HBCs were first purified from the hPSC-derived cells (day 9) by selecting attached cells on a human recombinant LN111 (BioLamina)-coated dish at 15 min after plating. The hPSC-derived HBCs were cultured on a human LN111-coated dish ($2.0 \times 10^4$ cells/cm$^2$) in maintenance DMEM/F12 medium (DMEM/F12 medium [Invitrogen] was supplemented with 10% FBS, 1 × insulin/transferrin/selenium, 10 mM nicotinamide, $10^{-7}$ M dexamethasone (DEX) (Sigma), 20 mM HEPES, 25 mM $NaHCO_3$, 2 mM L-glutamine, penicillin/streptomycin, 40 ng/ml hepatocyte growth factor [HGF] [R&D Systems] and 20 ng/ml epidermal growth factors [EGF] [R&D Systems]). The medium was refreshed every day. The hPSC-derived HBCs were dissociated with Accutase (Millipore) into single cells and subcultured every 6 or 7 days.

### Establishment and Maintenance of a Single hPSC-Derived HBC

For single-cell culture, the single HBC was plated to separate well of human LN111-coated 96-well plate in maintenance DMEM/F12 medium supplemented with 25 μM Y-27632 (ROCK inhibitor) (Millipore), and then colonies derived from a single cell were manually picked up and cultured as well as HBCs (these cells were designated the HBC clone).

### In Vitro Hepatocyte and Cholangiocyte Differentiation

To induce hepatocyte differentiation, the hPSC-derived HBC P0, HBC P10, and HBC clone were cultured for 14 days on a Matrigel-coated dish ($7.5 \times 10^4$ cells/cm$^2$) in HCM (Lonza) supplemented with 20 ng/ml HGF, 20 ng/ml Oncostatin M (OsM) (R&D Systems), and $10^{-6}$ M DEX. To induce cholangiocyte differentiation, the hPSC-derived HBC P0, HBC P10, and HBC clone were cultured in collagen gel for 14 days. To establish collagen gel plates, 500 μl collagen gel solution (consisting of 400 μl type I-A Collagen (Nitta gelatin), 50 μl 10 × DMEM, and 50 μl of 200 mM HEPES buffer containing 2.2% $NaHCO_3$ and 0.05 M NaOH) was added to each well, and then the plates were incubated at 37°C for 30 min. The hPSC-derived HBC P0, HBC P10, and HBC clone ($5 \times 10^4$ cells) were resuspended in 500 μl differentiation DMEM/F12 medium (differentiation DMEM/F12 medium was supplemented with 20 mM HEPES, 2 mM L-glutamine, 100 ng/ml EGF, and 40 ng/ml insulin-like growth factor 2 [ILGF2]), and then mixed with 500 μl of the collagen gel solution and plated onto the basal layer of collagen. After 30 min, 2 ml of differentiation DMEM/F12 medium was added to the well.

### Ad Vectors

Ad vectors were constructed by an improved in vitro ligation method. The human EF-1α promoter-driven FOXA2-expressing Ad vectors (Ad-FOXA2) were constructed previously (Takayama et al., 2012b). All of Ad vectors contain a stretch of lysine residue (K7) peptides in the C-terminal region of the fiber knob for more efficient transduction of hESCs, hiPSCs, mesendoderm cells, and definitive endoderm cells, in which transfection efficiency was almost 100%, and purified as described previously (Inamura

PH 48 hr were taken as 1.0. In (E), the gene expression levels in HBC P10 (before differentiation) were taken as 1.0. Data represent the mean ± SD from three independent experiments. Student's t test indicated that gene expression levels of the hepatocyte markers in "after" were significantly higher than those in "before" ($p < 0.01$).
(F) The efficiency of hepatocyte differentiation was measured by estimating the percentage of ASGR1-positive cells using FACS analysis.
(G) The amounts of ALB (left) and urea (right) secretion were examined. Data represent the mean ± SD from three independent experiments. Student's t test indicated that the percentage of ASGR1-positive cells, the ALB secretion level, and urea secretion level in "after" were significantly higher than those in "before" ($p < 0.01$).
(H) The procedure for the differentiation of the hESC-derived HBC P0, HBC P10, or HBC clone into cholangiocyte-like cells is presented schematically. Details are described in Experimental Procedures.
(I) Phase-contrast micrographs of the HBC P10-derived cholangiocyte-like cells are shown.
(J) The HBC P10-derived cholangiocyte-like cells were subjected to immunostaining with anti-CK7 (red) antibodies.
(K and L) The gene expression levels of hepatocyte (K) or cholangiocyte (L) markers in the HBC P0-, HBC P10-, or HBC clone-derived cholangiocyte-like cells were measured by real-time RT-PCR after 14 days of cholangiocyte differentiation. In (K), the gene expression levels in PH 48 hr were taken as 1.0. In (L), the gene expression levels in HBC P10 (before cholangiocyte differentiation) were taken as 1.0. Data represent the mean ± SD from three independent experiments. Student's t test indicated that the gene expression levels of cholangiocyte markers in "after" were significantly higher than those in "before" ($p < 0.01$). "Before" indicates the HBCs before hepatocyte or cholangiocyte differentiation; "After" indicates the HBCs after hepatocyte or cholangiocyte differentiation.
See also Figures S4 and S5 and Tables S1–S4.